UTILIZATION OF CHARACTERISTIC MODAL ANALYSIS FOR THE ANTENNA DESIGN NEEDED FOR AN AFIT SATELLITE

THESIS

Scott C. Podlogar, Captain, USSF

AFIT-ENG-MS-22-M-056

DEPARTMENT OF THE AIR FORCE
AIR UNIVERSITY

AIR FORCE INSTITUTE OF TECHNOLOGY

Wright-Patterson Air Force Base, Ohio

AFIT-ENG-MS-22-M-056

UTILIZATION OF CHARACTERISTIC MODAL ANALYSIS FOR THE ANTENNA DESIGN NEEDED FOR AN AFIT SATELLITE

THESIS

Presented to the Faculty

Department of Electrical and Computer Engineering

Graduate School of Engineering and Management

Air Force Institute of Technology

Air University

Air Education and Training Command

in Partial Fulfillment of the Requirements for the

Degree of Master of Science in Electrical Engineering

Scott C. Podlogar, B.S.E.E.

Captain, USSF

March 24, 2022

AFIT-ENG-MS-22-M-056

UTILIZATION OF CHARACTERISTIC MODAL ANALYSIS FOR THE ANTENNA DESIGN NEEDED FOR AN AFIT SATELLITE

THESIS

Scott C. Podlogar, B.S.E.E.
Captain, USSF

Committee Membership:

Andrew J. Terzuoli, Ph.D
Chair

Peter J. Collins, Ph.D
Advisor

Lt. Col. Michael D. Seal, Ph.D
Member

Ronald J. Marhefka, Ph.D
Member

Abstract

Antenna design is a pervasive knowledge base for electrical engineers. As the number of new materials and techniques increase, so too do the demand and requirements pushing forth new innovative ideas to expand the capabilities antennas can achieve. Characteristic Modal Analysis (CMA), originally credited to Garbacz and Turpin [1], is a leading edge analytic technique that is one of these ideas. CMA breaks down the current distribution along a structure in a way that can offer great insights into how that structure operates as an antenna. This technique has great merits in post design analytics and can be integrated into the design process. This thesis applies the techniques of CMA to create independent designs for a single antenna problem involving a AFIT Satellite. The results are three different designs that meet the requirements proving the utility of CMA in the antenna design process for this specific application.

Acknowledgment

I would first like to thank Dr. Collins for accepting the role of being my advisor. It was only with his guidance and teaching that this work was made possible. I also want to extend my gratitude to my other professors, Dr. Terzuoli and Dr. Havrilla, for taking the time to teach me everything I know about electromagnetism today. Lt. Col. Seal and Dr. Marhefka also played a big role as my committee members to help steer my research in the right direction when it started getting ahead of itself. Finally I like to thank my family for their support and encouragement throughout this difficult process.

Table of Contents

Page

List of Figures

List of Tables

UTILIZATION OF CHARACTERISTIC MODAL ANALYSIS FOR THE ANTENNA DESIGN NEEDED FOR AN AFIT SATELLITE

I. Introduction

1.1 Problem Background

In the last few years, technology in space including exploration, utilization and habitation has become a higher priority for the United States as evidenced by the creation of the United States Space Force. With the advancement of more efficient miniaturizing electronics, comes the natural progression of miniaturizing satellite components that can be designed with more capabilities in a smaller volume to reduce satellite launch costs [2]. A prototypical example of this is the development of the Cube Satellite (CubeSat). The CubeSat program can vary widely in their operation and structure but generally adheres to a standardized sizing table which allows for interchangeability with launch vehicles.

A particular mission objective determines a list of requirements. To meet all the requirements many design considerations need to be balanced. Examples of objectives can wildly range from collecting environmental data to relaying information securely. Almost all examples of mission objectives require some form of communication to either a ground base or another space vehicle. This is most successfully accomplished by utilizing an antenna.

The field of antenna design continually advances and there is already an immense amount of research on methods to meet various requirements. Antenna performance can be described by a vast amount of metrics including both radiation and spectral

properties. Radiation performance includes measures such as directivity, beam width, and power efficiency on a spectral basis. Spectral performance usually analyzes any particular metric over a range of frequencies, whether the requirement is met over a certain bandwidth around a target frequency or when a dual-band behavior exists. On top of that, physical characteristics of the antenna design, such as size and shape, are often important considerations that must be taken into account. Because of the vast variety of metrics that an antenna design could seek to optimize, it is often difficult to find a perfect pre-existing design for any novel set of requirements. This fact drives innovation and the discovery of new techniques in the field of antennas. When new ideas for manipulating electromagnetic fields are introduced, significant research is involved to leverage a particular design concept to improve the performance of existing designs.

1.2 Research Objectives

This thesis explores the design process for a specific antenna problem involving the AFIT Satellite and the considerations when using Characteristic Modal Analysis (CMA) in a variety of ways. One application examines using CMA in combination with an aperture coupled metasurface micro-strip antenna. Another application explores the technique of using the mounting structure as a radiator, utilizing CMA for proper positioning. The requirements include dual-band operation with two target frequencies; a lower frequency of 450 MHz for specific ground stations and a higher S-band frequency 2.285 GHz which is more typical for spacecraft communications. The bandwidth needed is only $\pm$ .25 MHz which is not difficult to achieve. Space is limited on the spacecraft as well as the launch vehicle therefore the profile of the antenna should not exceed 20 mm in height.

Although these requirements present a clear design challenge, the intent of the

Figure 1: This an image of the AFIT CubeSat project satellite to which this thesis refers to after a theoretical launch.

work presented is to highlight the utility of CMA and the influence it can have on design decisions as well as the theoretical understanding behind the antenna operation. The goal of this research is to present three different viable antenna solutions to the AFIT Satellite antenna problem which apply CMA principles in the design process. The purpose is to enhance the theoretical understanding behind antenna operation and provide insightful strategies for the antenna design process of the AFIT Satellite.

1.3 Document Overview

This thesis is structured into five chapters. The first chapter describes the problem statement and the research objective of this thesis. It provides the motivation and introduces the overall topic that is discussed. Chapter 2 presents all the background information that is required to understand the work, as well as the current research that has been done that relates to the problem statement. Next, the actual research conducted is presented in Chapter 3. It is split into three sections; CMA methods that

apply to a dipole antenna, the application of CMA to facilitate the development of a dual band microstrip metasurface antenna, and the application of CMA to position an antenna to utilize the antenna mounting structure for a dual band purpose. The results of each model presented in Chapter 3 are analyzed and discussed in Chapter 4. Chapter 5 summarizes the main findings and conclusions reached from this research. Recommendations for further research are also provided.

II. Background and Literature Review

This chapter reviews the prerequisite theory and methods used in this thesis. First, the concept of microstrip antennas is introduced and extended to metasurface design techniques. Then an overview of the derivation of Characteristic Modal Analysis (CMA) is presented. Finally the Literature Review Section highlights a selection of research that is particularly relevant to the problem statement. It also identifies many useful practices that will be applied to this specific example problem.

2.1 Microstrip Antennas

The microstrip antenna design, sometimes referred to as a "patch" antenna, is usually preferred for high performance vehicles, compact devices, or applications that need to optimize space. A basic microstrip antenna consists of a metallic (often copper which is modeled as a Perfect Electrical Conductor (PEC)) strip, or "patch", elevated above a ground plane (see Figure 2). Usually a layer of dielectric material separates the strip from the ground plane. The strip requires a feed structure to create a potential difference between it and the ground plane which will form the electromagnetic waves.

Microstrip antennas are used because the vertical profile can be on the order of millimeters. They can also be flexible and conform to non-planar surfaces. However, there are operational disadvantages compared to simple antenna designs like dipoles which include low efficiency, low power, poor polarization purity, poor scan performance, spurious feed radiation and very narrow frequency bandwidth [3]. The next section discusses the various feed structures that are commonly used and their tradeoffs. This is relevant as CMA design decisions are often tied to the type of feed and its placement.

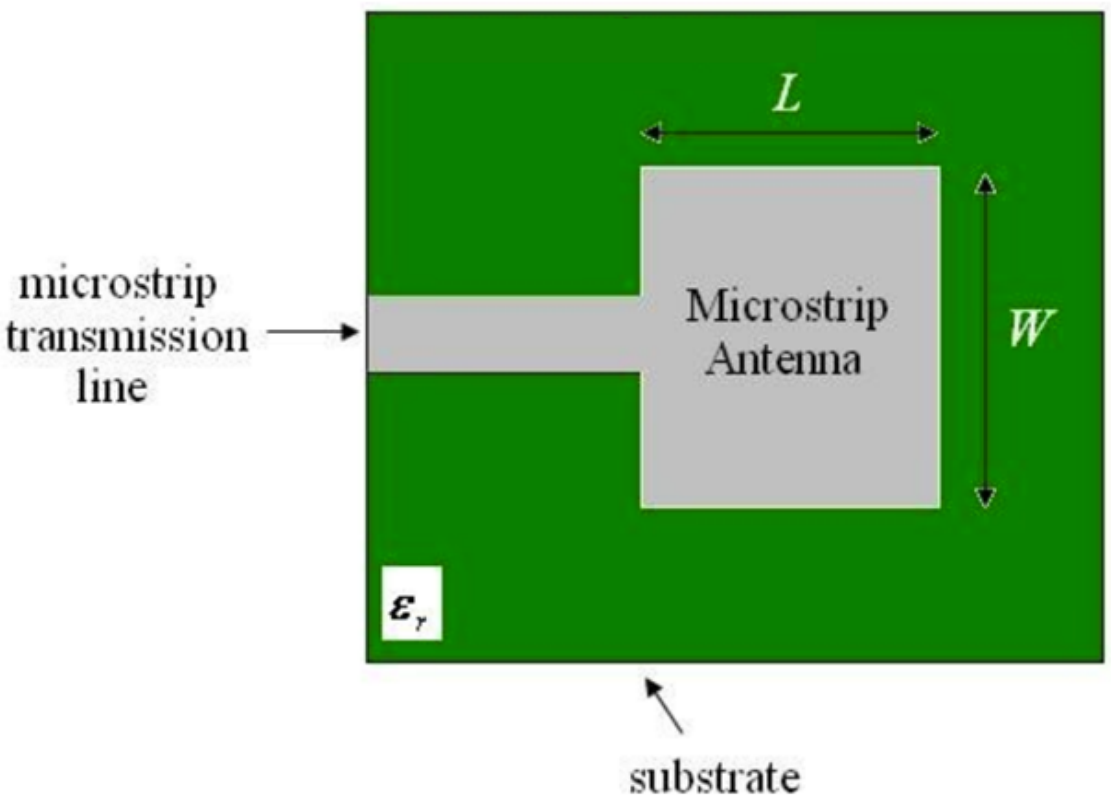

Figure 2: This is the top view of a basic microstrip antenna. It illustrates how a patch antenna can be a simple geometry such as a square but needs an excitation source. In this case, it is the microstrip transmission line adjacent to the patch [4].

The shape of the patch directly determines the operating frequency of the antenna. Simple geometries such as rectangles and circles are common because they are easier to analyze. The electrical size of the patch drives the resonate frequency. This can create a problem for lower target frequencies when space is a factor as a larger size is necessary. Raising the relative permittivity of the dielectric can mitigate this issue by relaxing the physical size of the patch but usually a lower permittivity value is desired. Lower permittivities have wider fringes and therefore better radiation with increased bandwidth as well as increased efficiency [4]. The length (the dimension in line with the feed) of a rectangular patch can be expressed in terms of the operating

frequency approximately as

$$L = \frac{1}{2f\sqrt{\epsilon_0 \mu_0 \epsilon_r}}$$

Increasing the height of the substrate can increase the bandwidth but also creates traveling waves that travel within the substrate and thus create undesired radiation that may couple to other components. The height of the substrate should still be significantly less than the operating wavelength but greater than about $1/40^{th}$ of the wavelength or the efficiency will degrade [4]. There are many methods for thoroughly analyzing microstrip antennas including the transmission-line, cavity, and full wave model [3]. However, when these methods are applied to more complex antennas, rigorous analyses may become too complex for initial design work and is outside the scope of this thesis. The general principles previously explained is sufficient in the initial design of the antenna.

2.1.1 Feed Structures

When designing an antenna, one of the most important considerations is how the antenna will be excited electrically by the feed structure as the design can introduce inefficiencies. For microstrip antennas, a feed line could come from the side, referred to as an inset feed, or could come from underneath the patch, referred to as a probe feed. The feed line could even avoid contact with the patch and instead use electric fields to create the excitation by means of coupling. See Figure 3 for an illustration of each feed technique. Feeding the patch directly along the surface is usually preferred in terms of performance. Although it leaves less room for radiation in undesired direction, feeds from the bottom are often more practical to implement physically. The probe feed also has the potential to introduce unwanted inductance depending on the height of the substrate [4]. One of the best feed techniques to use in a CMA based design approach is the aperture coupling method. With this method there are three layers;

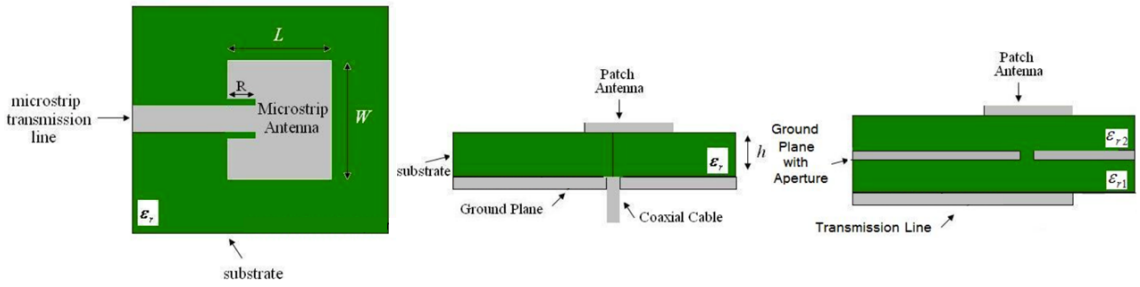

Figure 3: These are three different feed structures for a microstrip antenna. From left to right they are an insert feed, probe feed, and aperture coupling [4].

the transmission line layer, the ground plane, and the radiation surface. The layers are separated by a substrate with a given height and relative permittivity. The lower substrate has a higher relative permittivity and is thin enough to mitigate spurious radiation. Conversely, the upper substrate is usually a lower relative permittivity to produce loosely bound fringing fields, yielding better radiation [4]. The ground plane generally acts as an electrical shield for the radiation surface from the transmission line. However, there is an aperture in the ground plane which allows the generated fields from the transmission line to pass through and excite the radiation plane. This feed technique is common with CMA because it allows for broad customization of the excitation field from the transmission line which will excite surface current distributions. This concept is reviewed again later in the section 2.3.3 which covers how CMA can be used for design.

2.2 Introduction to Modal Analysis

Antenna designs can be evaluated via computational numerical methods, such as Method of Moments (MoM), finite-difference time domain (FDTD), and Finite Element Method (FEM) all of which can be used to analyze the design and predict the radiation characteristics. Some common examples of software that employ these methods include Mercury MoM, CST Microwave Studio, and FEKO [5][6]. The anal-

ysis performed in this thesis used FEKO's simulation software with a MoM solver. The technical derivations of of MoM is covered in section 2.3.1. These numerical methods are powerful and allow experienced antenna designers to find a reasonable design or to optimize their design by iteratively using a solver as design parameters are varied. However, the results of these brute force iterative searches, especially for inexperienced antenna designers, can sometimes lead to complex designs that are difficult to analyze by non-numeric means. Modal analysis techniques can arrive at similar solutions but offer more information that describes the antenna operation.

The most common modal analysis techniques used for antenna engineering include spherical mode, dielectric waveguide model, and the cavity model [3]. The cavity model is used specifically for the analysis of microstrip antennas, whereas the dielectric waveguide model focuses on the analysis of waveguides while the spherical mode only works for electrically small antennas. In cavity model theory, the microstrip antenna is modeled as a lossy resonant cavity when there are uniform fields and the model is bounded by electric boundaries on the top and bottom and magnetic walls along the perimeter (See Figure 4). The theory states that the fields underneath the patch can be expressed as the sum of various resonant modes which take the important fringing fields into account. More in-depth and rigorous explanations of this analysis technique exist but are not covered in this thesis [3]. This method only works for very thin electrical substrates since thicker substrates allow for surface waves to propagate within the substrate which violate the uniform field assumption. In summary, the modal techniques reviewed in this thesis work well for most situations but there are specific antenna problems that it can not handle which becomes the motivation behind CMA [7]. The microstrip antenna is the focus of this thesis because of the advantages of its low physical profile to which it can operate although this comes with tradeoffs in performance. There are design techniques such as capacitive coupling feed, stacked

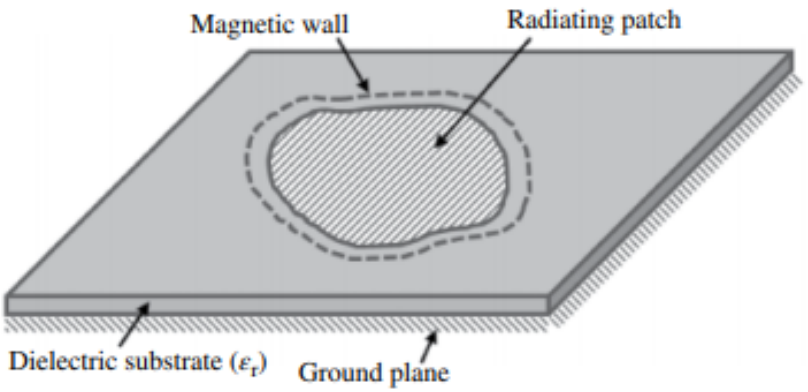

Figure 4: This is an illustration of the key characteristics of the Cavity Model which is used to analyze a patch antenna. A rigorous analysis can be found in the Balanis text book [3].

patches, thick air substrate, parasitic resonators, and reactive slot loading which attempt to improve the bandwidth but usually at the cost of physical size [8]. Another technique that is examined in this thesis is metasurfaces, which refers to engineering the surface of the antenna to a shape or pattern.

There are various theories or strategies on what drives the design of a metasurface for a given set of requirements. These include effective medium theory, equivalent circuits, transmission and reflection coefficients calculation under normal incidence of a plane wave, modal dispersion curve, and surface impedance extraction [9]. CMA is a more accurate technique in antenna design on the scale of the target antenna because other methods rely on the infinite periodic boundary approximation which is inaccurate with a model that has a small number of unit cells. This approximation does not allow for modeling antenna radiation problems where the metasurface is tightly coupled to its primary source, as is the case for the microstrip antenna design being considered in this study [9].

2.3 Characteristic Modal Analysis

The premise of CMA begins with the simple understanding that current running through/on an object can produce an electric field. Put mathematically,

$$L(\vec{J}) = \vec{E}$$

where L is a linear operator, $\vec{J}$ is a vector field of an arbitrary current on an object and $\vec{E}$ is the vector field of the electric field produced by that current. For example, the electric field from current impressed on a PEC follows this equation where L is defined as [7]

$$L(\vec{J}) = \vec{E}(\vec{r}) = \frac{jk_0\eta_0}{4\pi}\left(\int_S \vec{J}(\vec{r'})G(\vec{r},\vec{r'})dS' + \frac{1}{k_0^2}\nabla\int_S \nabla'\cdot\vec{J}(\vec{r'})G(\vec{r},\vec{r'})dS'\right)$$

and where the Free Space Green's Function is defined to be

$$G(\vec{r},\vec{r'}) = \frac{e^{-jk|\vec{r}-\vec{r'}|}}{|\vec{r}-\vec{r'}|}$$

The derivation for the L operation is complex and utilizes Maxwell's Equations, Vector Potentials and proper boundary conditions with a certain set of constitutive parameters. The information about the radiating body geometry is also contained in the L operator. This can be seen in the equation above through the use of the surface integrals which integrate over the surface of the radiating body. In other words, the geometry of the body defines the boundaries of the integral and hence is an input to the L operator. However, the example is of a PEC and that a non-PEC would have more complex boundary conditions leading to volume integrals in the L operator.

Before going into the derivation of the CMA, it is necessary to review the MoM derivation. Computer simulations rely on numerical methods to arrive at approxi-

mations which can be quite accurate even when the problem is too complex for an analytic solution. Since the simulation requires a numerical formulation, it is appropriate to explain how CMA is applied to that numerical formulation. As MoM was the exclusively used numerical method for the results in this paper, it is worth reviewing the derivation.

2.3.1 Method of Moments

In the classic scattering problem, the scattered electric field along the boundary of an object is known and the equivalent current that produced the field is desired. This presents a problem though in solving for the current as the inverse of the L operator from the equation in the previous section, $\vec{J} = L^{-1}(\vec{E})$, is not easily found.

This is where numerical techniques come into play, one of which is MoM. It aims to approximate the evaluation of the L operator as a transformation matrix by discretizing the equation $L(\vec{J}) = \vec{E}$ and forming the matrix equation $\mathbf{ZJ} = \mathbf{V}$ whose derivation is explained below. The matrix equation $\mathbf{J} = \mathbf{Z}^{-1}\mathbf{V}$ is solvable though may be computationally intensive requiring a large amount of computing power to solve depending on the size of $\mathbf{Z}$.

Start by having a component of $\vec{J}$, an arbitrary current distribution, take the form

$$\sum_{n=1}^{\infty} a_n f_n$$

where a_n is a weighting coefficient and f is a set of orthogonal basis functions. Some example basis functions include a pulse basis set like $f_n = u(x-n)\Delta x$ and a polynomial basis set such as $f_n = x^n$. Figure 5 illustrates this by using a set of three pulse basis functions to approximate a signal function. It is easily inferred that the approximation accuracy will increase with the number of basis functions. Also notice how the basis functions alone contain no information and it is the weighted coefficients that

carry the data corresponding to the signal. These examples are only one dimensional to demonstrate their simplicity where in most applications a three dimensional variant is necessary to model the three dimensional vector current. The point being that an infinite number of basis functions weighted appropriately can model any function. Truncating the sum to a finite number of basis functions discretizes $\vec{J}$.

$$J_x = \sum_{n=1}^{N} a_n f_n$$

where J_x is the x dimensional component of $\vec{J}$ and can be represented as a N x 1 column vector. The information that defines J resides in the weighting coefficients rather than the basis functions as the basis functions are chosen and not derived. The weighting coefficients are separated out so that J is a simple N x 1 column vector of coefficients that could be used to construct an approximation of J in conjunction with the basis functions.

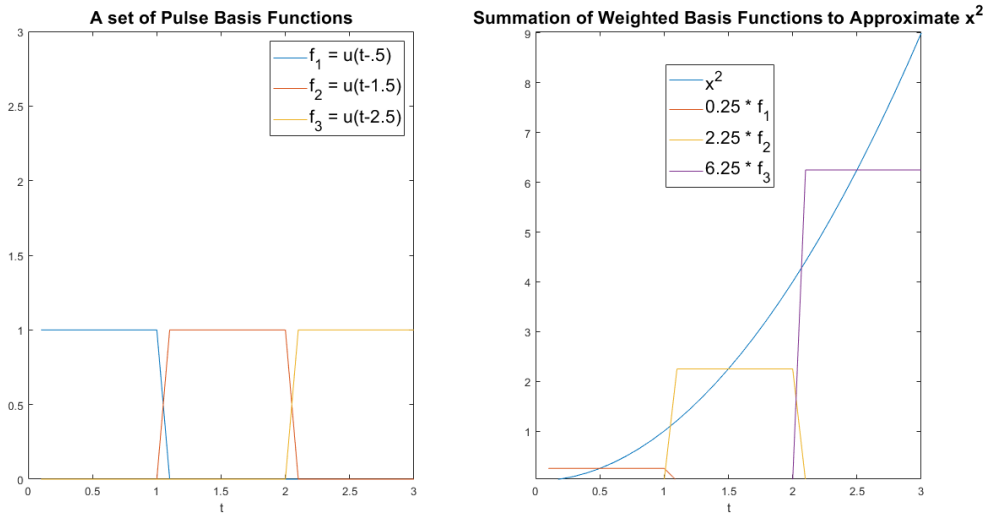

Figure 5: An illustration of $J \approx \sum_{n=1}^{3} a_n f_n$ with $f_n = 1$ for $n - .5 < t < n + .5$ and $a_1 = 0.25, a_2 = 2.25, a_3 = 6.25$. This example shows how a weighted set of basis functions can approximate other meaningful functions.

Substituting in the approximation form of J into the original equation gives

$$L(\sum_{n=1}^{N} a_n f_n) \approx \ E$$

which, given that L and summation are linear operators, can then become

$$\sum_{n=1}^{N} L(f_n) a_n \approx \ E$$

The sum can take the form of a produte of two vectors. One is a row vector with dimensions 1 x N and the other is a column vector that is N x 1 which comprises of the weighting coefficient that is factored out. The first term takes the form of

$$\mathbf{Z}_1 \ = \ [L(f_1) \ \ L(f_2) \cdots L(f_N)]$$

and the overall equation can simplify to $\mathbf{Z}_1\mathbf{J} \approx E$. The electric field in the original equation is a continuous function but when the current is discretized and becomes an approximation, the resulting electric field becomes an approximation to the true continuous electric field. The electric field must also be discretized which can be done by sampling the field through the use of an inner product. For instance: $\langle t_m, \mathbf{Z}_1\mathbf{J} \rangle = \langle t_m, E \rangle$ where the inner product and testing functions are chosen; a common type example being $\langle t_m, E \rangle \ \equiv \ \int_V t_m E dV$ and $t_m \ \equiv \ \delta(x-m)\delta(y)\delta(z)$ [10]. N testing functions are usually chosen which can then be stacked into a matrix with each row representing a test function equation. Finally, given that inner products are linear, J can be separated and the equation takes the form,

$$\mathbf{ZJ} = \mathbf{E}$$

where $\mathbf{Z}$, referred to as the impedance matrix, has the elements $Z_{nm} = \langle t_m, L(f_n) \rangle$

and $\mathbf{E}$ is a sampled vector of the continuous E. The elements of the impedance matrix are independent of the actual current as the basis functions used to define the current do not actually contain any information without their corresponding weighting coefficients. However, the elements still use the L operator which, as explained in the previous section, does depend on the geometry of the radiating object.

The goal of this process is to approximate the L operator as a transformation matrix that becomes independent of its input. This new transformation matrix, known as the impedance matrix, is dependent only on the geometry of the radiating object and the given operating frequency. While usually the impedance matrix is used to solve for the electric field given a current distribution, in CMA, the impedance matrix itself can also be analyzed to determine the modal structures of the modeled geometry.

2.3.2 Characteristic Modal Analysis Derivation

Eigenvalues may be derived from a given matrix, with each eigenvalue is an associated eigenspace whose basis vectors are referred to as eigenvectors. The eigenvectors are those that only scale when the transformation matrix is applied as opposed to being transformed. Reframing the application to fit electromagnetics, eigenanalysis can be performed on the impedance matrix to solve for eigenvectors. However, as currents are the acceptable pair to impedance matrices, the derived eigenvectors are represented as $\mathbf{J}_n$ where n is n^{th} eigenvalue. The formula which defines eigenvalues then becomes [7],

$$\mathbf{Z}\mathbf{J}_n = \nu_n \mathbf{W}\mathbf{J}_n$$

where ν_n is the n^{th} eigenvalue and $\mathbf{W}$ is a suitably chosen matrix that will diagonalize $\mathbf{Z}$. Since $\mathbf{Z}$ could be complex it can be represented as

$$\mathbf{Z} = \mathbf{R} + \mathbf{X}j$$

where

$$\mathbf{R} = \frac{\mathbf{Z} + \mathbf{Z}^*}{2}, \mathbf{X} = \frac{\mathbf{Z} - \mathbf{Z}^*}{2j}$$

Picking $\mathbf{W} = \mathbf{R}$ and letting $\nu_n = 1 + j\lambda_n$, the equation becomes $(\mathbf{R} + j\mathbf{X})\mathbf{J}_n = (1 + j\lambda_n)(\mathbf{R})\mathbf{J}_n$. Since $\mathbf{R}$ and $\mathbf{X}$ are both real, the imaginary and real parts can be equated to,

$$\mathbf{R}\mathbf{J}_n = \mathbf{R}\mathbf{J}_n$$

$$\mathbf{X}\mathbf{J}_n = \lambda_n \mathbf{R}\mathbf{J}_n$$

It is then straightforward to solve for the eigenvalues, λ_n, with the corresponding eigenvector currents which are also referred to as the characteristic currents as they are a set of currents that are characteristic of the geometry of the object. These characteristic currents can be shown to be orthogonal meaning that [7],

$$\langle J_m, Z J_n \rangle = \begin{cases} 0 & m \neq n \\ \nu_n & m = n \end{cases}$$

This means they can form a basis set of their own that can be used to define a realized current. Much like the technique used in MoM, the current can be represented as

$$J = \sum_{n=1}^{N} J_n a_n$$

using the set of characteristic currents as a basis which when substituted into the equation $\mathbf{ZJ} = \mathbf{E}$ takes the form,

$$\sum_{n=1}^{N} (ZJ_n)\, a_n = E$$

Now using the fact that the characteristic currents are orthogonal and the principles of linearity for inner products and summations, taking the inner product of both sides will isolate the Modal Weighting Coefficient (MWC) [7],

$$\langle J_m, \sum_{n=1}^{N} (ZJ_n)\, a_n \rangle = \langle J_m, E \rangle$$

$$a_m \nu_m = \langle J_m, E \rangle$$

$$a_n = \frac{\langle J_n, E \rangle}{|1 + j\lambda_n|}$$

The MWC is a product of two terms; the Modal Significance (MS),

$$MS = \frac{1}{|1 + j\lambda_n|}$$

and the Modal Excitation Coefficient (MEC),

$$MEC = \langle J_n, E \rangle$$

The MEC is a measure of how well coupled the electric field is to the particular characteristic mode. Through reciprocity the derivation remains unchanged for an incident electric field inducing current on the object. In this sense the excitation coefficient can be seen as how closely the incident electric field will excite that particular characteristic current. This is very relevant in designing the feed of an antenna. The MS, on the other hand, is independent of any excitation and is only dependent on

the geometry. It ranges from 0 to 1 and is a measure of the coupling capability of each mode. Given a simple antenna such as a dipole designed to operate at a certain frequency, one particular current mode will resonate better than all the other current modes that the dipole can support at that operating frequency. This can be shown by the MS for that modal current at that frequency being nearly one where all the others are much lower signifying resonance.

Another metric that is often referenced in terms of characteristic modes are the characteristic angles. The set of characteristic currents each create a characteristic electric field that contains a component that is tangential to the surface of the body. This tangential component is equiphase all along the body and contains a phase lag with its corresponding characteristic current [7]. This phase lag is referred to as the characteristic angle and is easily calculated from the characteristic eigenvalues by the following

$$\theta = 180^\circ - \tan^{-1} \lambda_n$$

Resonance is easily shown in a graph of characteristic angles as the frequency that gives the value of 180°. The characteristic angle also provides a reference to compare the phases of characteristic currents. Obtaining two modal currents that are 90° off in phase is often a goal when trying to create a circular polarization. Circular polarization is especially important for space based communications as it can penetrate Earth's ionosphere more efficiently.

2.3.3 Designing with Characteristic Modal Analysis

There are two major ways of applying CMA when designing an antenna. The first way is applicable when mounting a smaller antenna element to a mounting structure. Lower frequencies correspond to larger wavelengths which smaller antennas will have a difficult time capturing. However, it may be possible to utilize the mounting structure

itself as the antenna and to use the antenna element as a feed. The mounting structure would have to be sized similar to the target wavelength and be able to conduct current to radiate electric fields. Using CMA on the mounting structure will reveal what current modes the structure can support and the MS of each mode at a particular frequency. If there proves to be a desirable characteristic mode that has a higher MS, the antenna element can be placed in a way that will maximize the MEC for the desired mode.

CMA can also be applied to tailor a metasurface antenna for a more precise radiation pattern. It can be used to examine the weight of all the characteristic currents contributing to the radiation of a microstrip antenna. By separating out the characteristic currents, designers can determine which modes are beneficial and which modes should be suppressed. Modifications can then be made to the metasurface such as resizing or cutting away patches that will alter the MS. Much like the previous technique, the feed for the microstrip antenna can also be optimized to excite only the desired modes.

2.4 Literature Review

The methods and principles used in this thesis have been researched and applied in many different ways. A paper published by Yi Zhao utilizes metasurface microstrip antennas with an aperture coupled feed that is designed for circular polarization [11]. Zhao demonstrates that when the aperture is rotated off the main dimensions of the microstrip patch, a circularly polarized radiation pattern is created (see Figure 6 for the results). The concept is validated by realizing an axial ratio below 3dB at the operating frequency. This use of the aperture positioning is used and expanded upon by most of the articles featured in this section. Zhao also discusses the use of an array of rectangles which is another common element in microstrip antennas.

Other publications highlight modifications to the metasurface design to introduce capacitive loading which, in turn, modifies the axial ratio and reflection coefficient to a more desired outcome [12]. Collectively, these studies demonstrate common feed structures and radiation characteristics of certain patterns that are necessary for designing a metasurface antenna. However, these papers do not explain the how the initial metasurface design is chosen. Without more information concerning the process of selection, subsequent modifications of the design for different requirements are difficult. The CMA techniques demonstrated in this thesis can be applied to these antenna designs and extend the understanding of how changing metasurfaces affects performance and thus contribute to a more flexible design process. Another paper written by Feng Han Lin and Zhi Ning Chen examines a very similar antenna design [9]. Lin's and Chen's paper uses CMA with a design process that includes a ground slot and cuts on the metasurface to promote the desired characteristic currents, (see Figure 7 for the design). Although there is no concern about polarization or multiband performance, this design procedure is a useful example of how to apply CMA.

Francesco Dicandia and Simone Genovesi demonstrate the utility of CMA in the post analysis of their antenna design [13], which includes a space based application that aligns closely to the goals of this thesis, (see Figure 8 for the antenna design and results). The authors used CMA to demonstrate how these modifications to a standard patch array metasurface create the desired axial ratio. More specifically, Dicandia and Genovesi show how the characteristic angles of the chosen modes are approximately off by 90° at the operating frequency which leads to a strong circular polarization shape. The paper also includes a sensitivity analysis to explain the effects of the ground slot, the finite ground plane, and the non-uniform pattern of the metasurface on the characteristic currents.

Another paper co-written by Chen explains the design of a dual band antenna

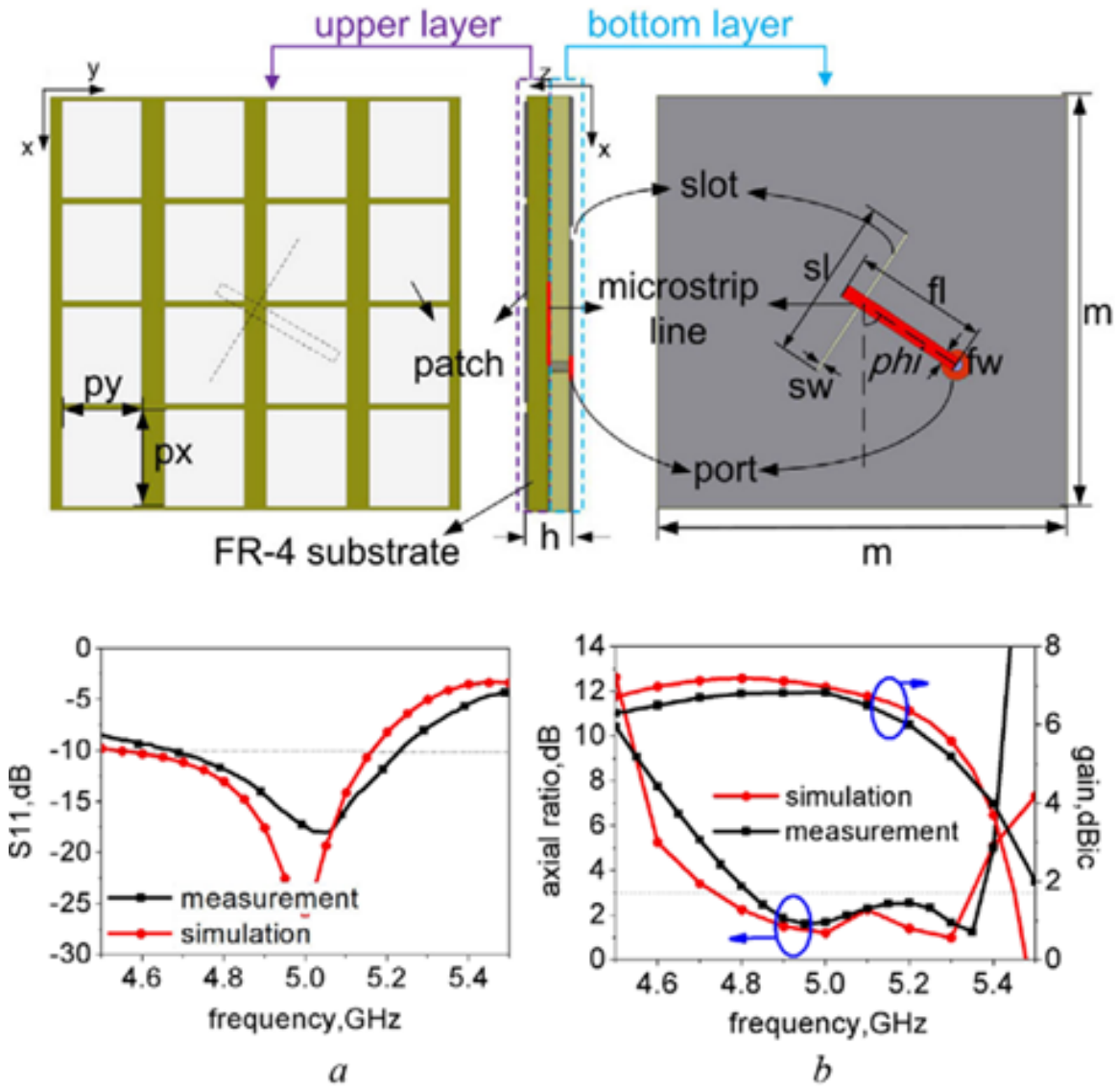

Figure 6: A standard array of patches can form a simple metasurface. The aperture coupled feed structure is angled to produce circular polarization effects. The results show a low reflection coefficient and low axial ratio at the operating frequency validating the design [11].

designed with CMA [14]. Unlike other examples, Chen uses CMA and modifies the metasurface to suppress unwanted modes. The first section describes how a simple patch array has characteristic modal currents that will support radiation from 27-43 GHz although only the target frequencies 28, 33, and 36 are desired. For this case, the modifications to the metasurface act to reduce the significance of the modes that

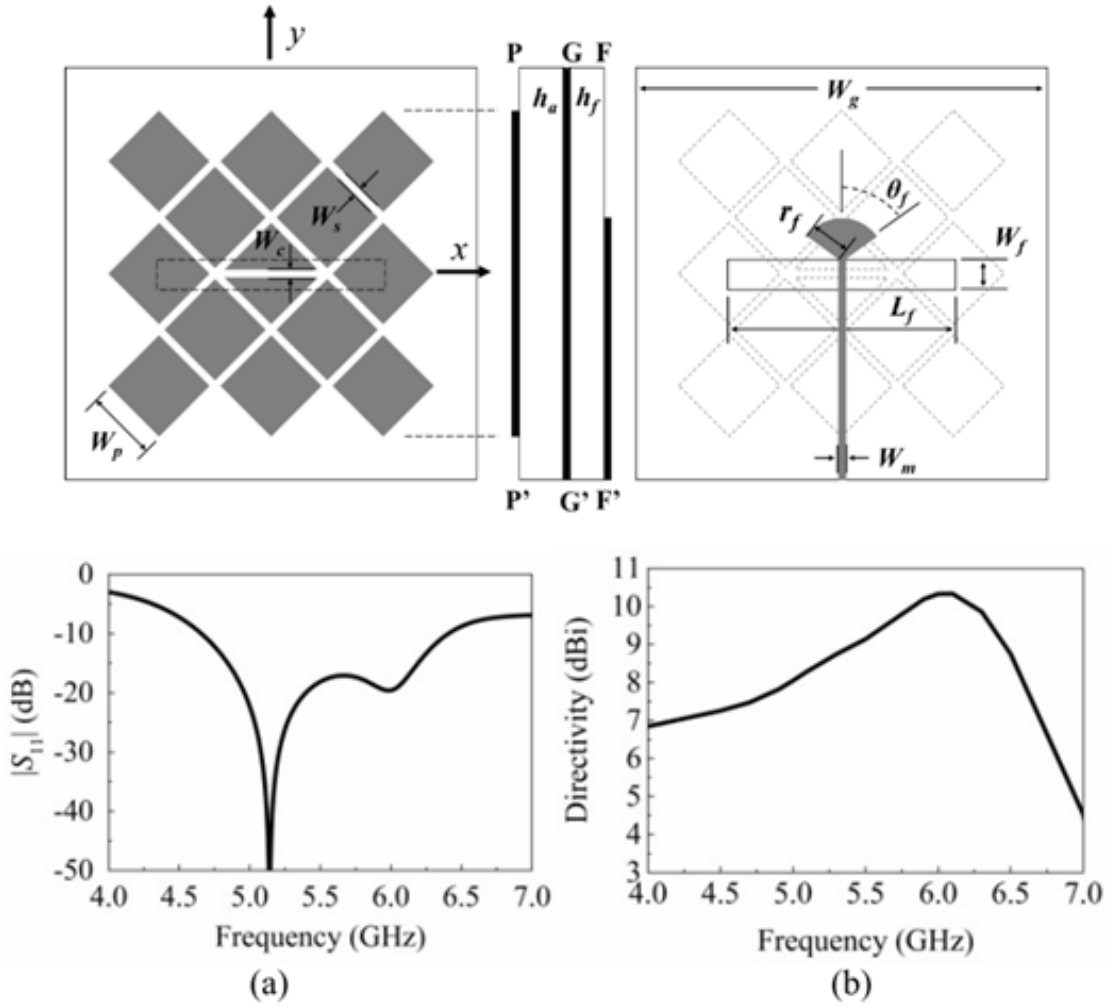

Figure 7: The top image shows the antenna design which is similar to the previous examples. The S_{11} parameter and directivity are shown in graphs a and b respectively to validate the operation of the design [9].

resonate outside the target frequencies and thus create the dual band behavior, see Figure 9. However, the range between the target frequencies of this thesis, 450 MHz and 2.285 GHz, is far more drastic than those used by Chen. It is discussed in Chapter III that the antennas considered in Chen's study can not easily achieve characteristic currents that support both target frequencies like they do with this application. Chen assumes that a simple design that supports modes in the desired frequency spectrum is already conceived of and thus, does not explain how to arrive there as it is not

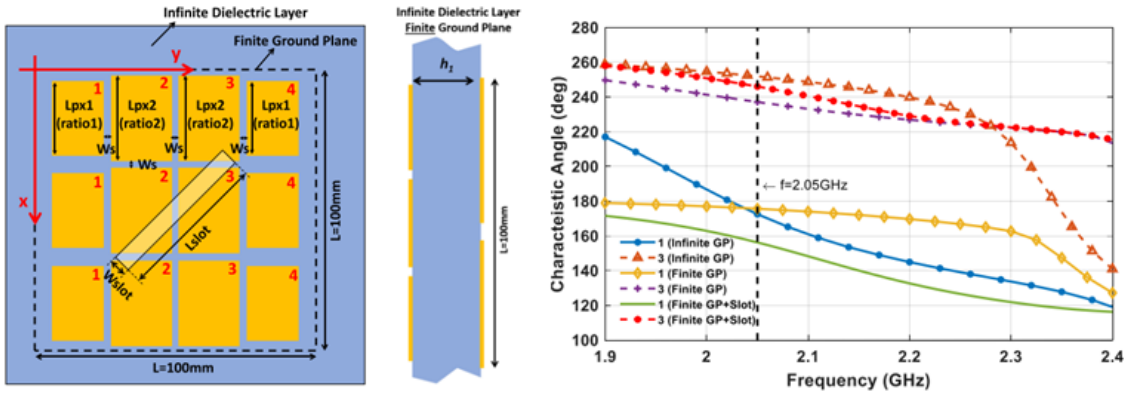

Figure 8: A similar antenna design to the one done by Zhao [11] but this one illustrates the use of Characteristic Angles from a CMA point of view to explain the axial ratio result [13].

necessary to his topic [14]. The methods used to curtail modes are still valuable and are also emphasized in a paper written by Feng Han Lin [15], which Chen also co-authored. Lin places emphasis on how suppression of unwanted modes increases the efficiency of the radiation of the proposed antenna [15].

CMA can also be employed during antenna placement, especially when a low target frequency is desired but the size of the antenna is also limited. For optimal antenna placement under these conditions, the mounting structure of the antenna is set to a low target frequency and acts as the radiator itself to which current along the body must be of the antenna element. By using CMA on the mounting structure itself, the characteristic currents that emit the desired radiation effects can be isolated and excited independently with proper antenna placement. Newman, describes this process with a simplified model of an airplane and how, with proper placement, the radiation efficiency at the target frequency is greatly improved (see Figure 10 for the results) [16].

Another paper by Martin Vogel, follows Newman's same procedure with a much more detailed model of an airplane. Vogel analyzed his airplane model with CMA

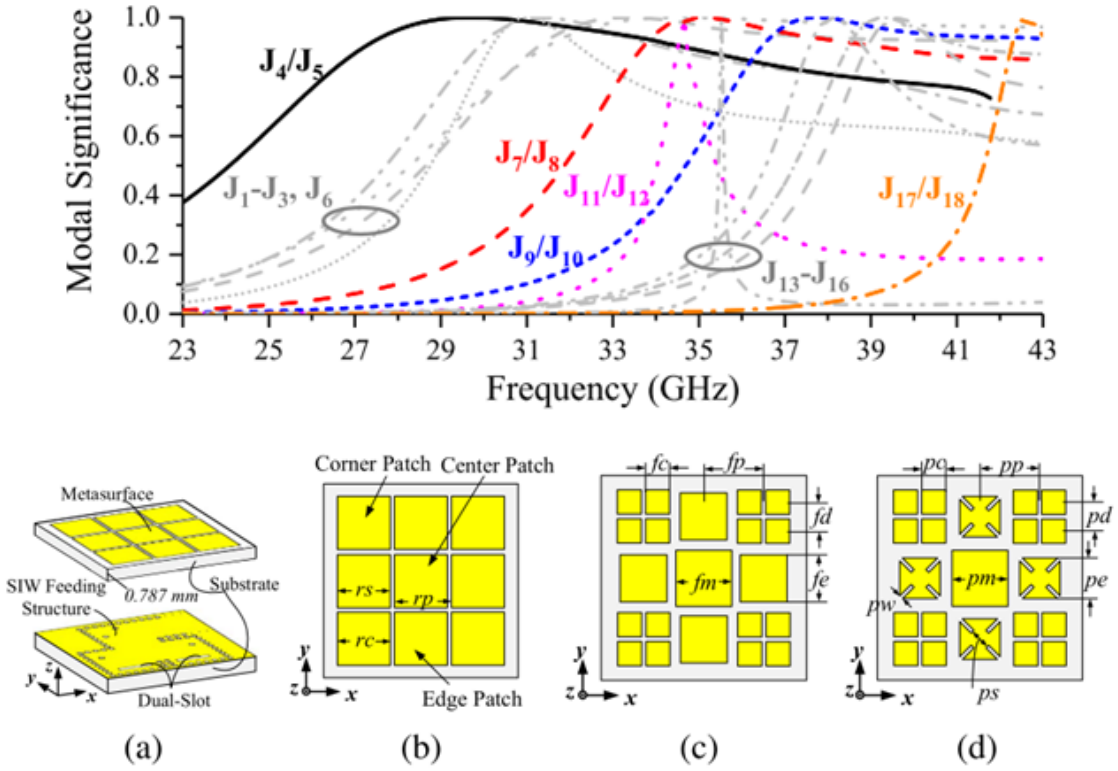

Figure 9: The top graph shows all the characteristic current modes that can be supported by antenna (b). The highlighted modes are desired and the others are suppressed by the modification shown with design (d). (a) shows a three dimensional view of the feed structure while (b)-(d) show the design evolution to suppress certain current modes [14].

and the first three significant modes are featured here (see Figure 11) [17]. Using the results of the CMA, specific antenna positions were identified to be optimal to resonate with the desired modes. The initial results of these antennas showed reflection coefficients nearly equal to one, indicating poor antenna efficiency (see Figure 12). Vogel explains that once the antennas were modified to match the input impedance the results improved and that the optimal placement of the antennas using CMA increased the operational bandwidth. However, this claim, which seems to be the main purpose of the article, shows no evidence nor applies any theory to explain his findings. The only evidence Vogel provides is a graph of the reflection coefficient of

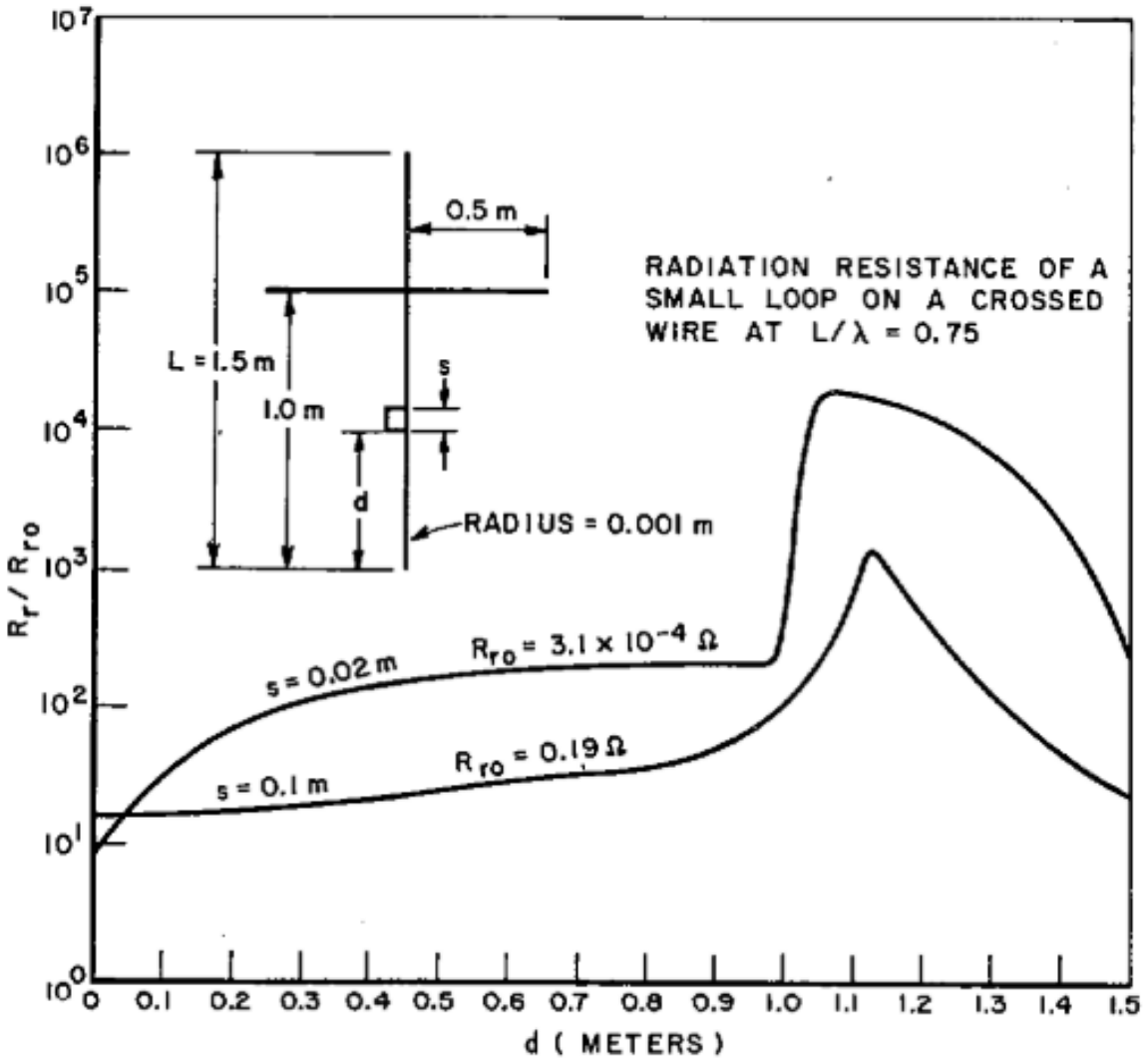

Figure 10: This graph shows that there is an optimal positioning for a small loop antenna on a large cross wire frame. The radiation resistance, (the value that when maximized provides maximal radiation efficiency) is optimal just above the intersection on the wire frame [16].

the "optimal" positioned antennas without any non-optimal placements.

In summary, several articles use metasurface designs that explain characteristics of a design with CMA and use CMA for optimal placement of antennas. All of these sources are important for this research. This thesis utilizes and extends principles demonstrated in the literature as they apply these techniques to a different unique problem.

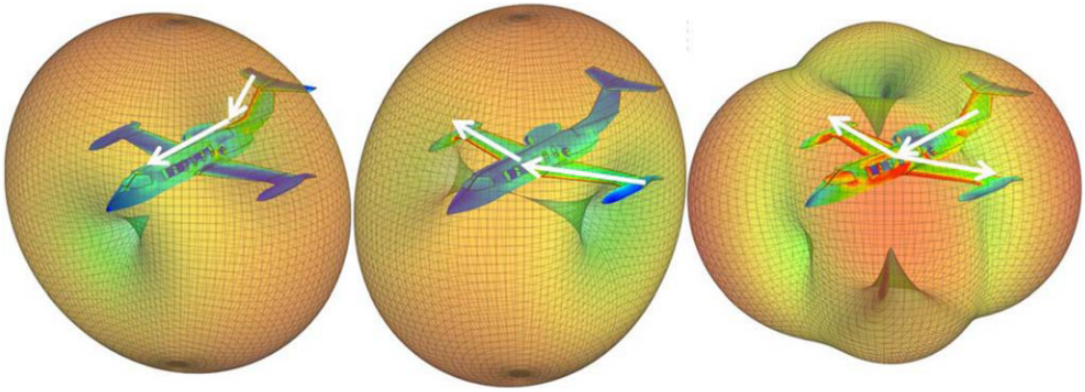

Figure 11: The images above are visualizations of the first three characteristic current distributions and characteristic electric fields that have a high MS at the operational frequency for the aircraft's geometric body. The white arrows and the heat map indicate current while the contour cloud is the excited electric field [17].

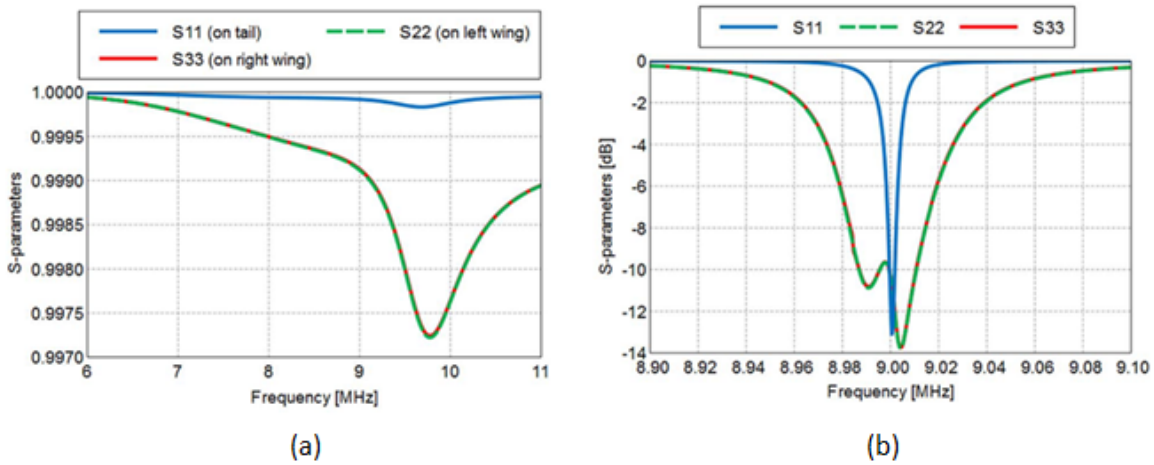

Figure 12: Sub-figure (a) shows the reflection coefficient is close to one even when CMA was used for optimal placement. Sub-figure (b) shows the same setup but for when the ports were adjusted to match the input impedance [17].

III. Methodology

3.1 Introduction

This chapter focuses on the methodology for three separate approaches to designing an antenna using Characteristic Modal Analysis (CMA). The first application is centered around a dipole antenna. This serves to not only validate CMA with a simple, well known antenna model but allows for an easy introduction into how CMA can be applied in the design process. The next application shows how CMA can be used to gain insight of the currents on the surface of a patch antenna. Finally, the last application explores how CMA can be used to encourage radiation of an antenna mounting structure. All three applications demonstrate an antenna design and configuration that operates at 450 MHz and 2.285 GHz in the vicinity of the Cube Satellite (CubeSat). The following chapter compares, contrasts, and individually analyzes the benefits and drawbacks of the three discussed applications.

3.2 The Dipole Application

Before using any new antenna design method it is a good idea to validate the theory on a known example such as a simple dipole. This section describes the full breakdown of the CMA and the radiation characteristic of a dipole that is 2 m long, has a 2 mm radius, is center fed with a voltage source and is analyzed in the frequency range of 60 MHz to 260 MHz. Analytic and numerical solutions, which are both quite extensive and well accepted, show a strong resonant behavior at 72 MHz and 220 MHz. Figure 13 shows the reflection coefficient vs. the frequency that supports those claims. For this example, the Modal Significance (MS) of the antenna without the source is considered and then the Modal Excitation Coefficient (MEC) is used to examine the effect of the source location. Finally the implication of the Modal

Weighting Coefficient (MWC) is then discussed.

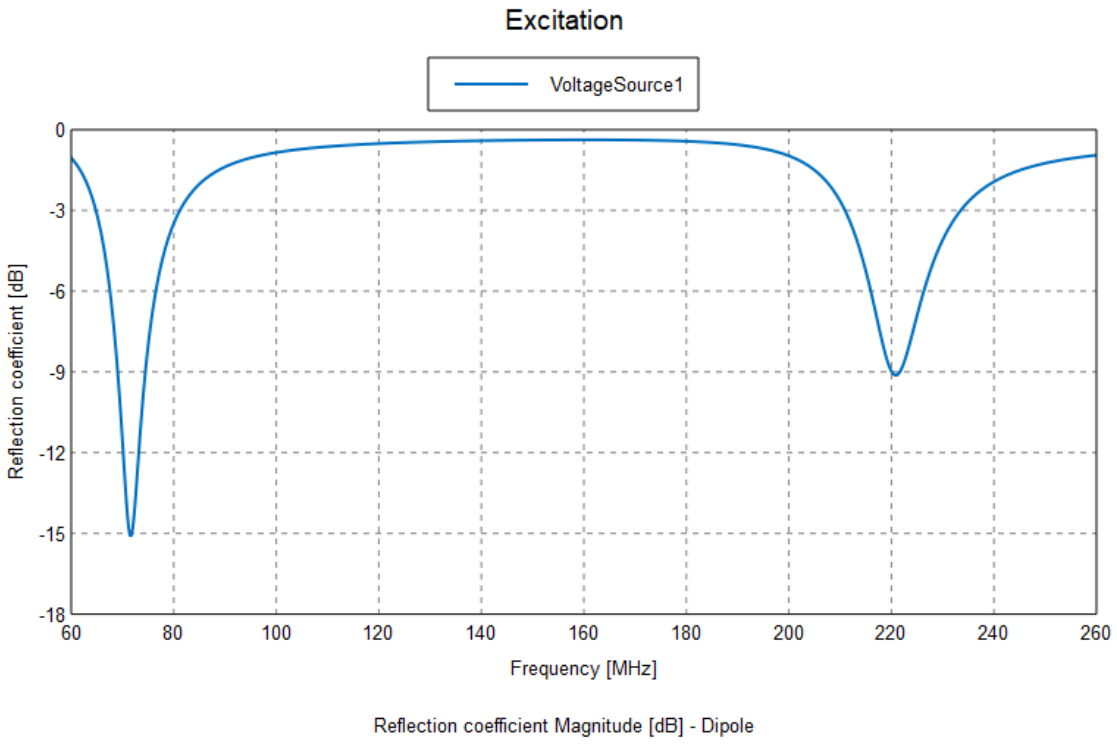

Figure 13: The reflection coefficient of the center fed dipole antenna as a function of frequency. There are two clear operating frequencies at 72 MHz and 220 MHz.

3.2.1 Modal Significance

The code that performs CMA for Feko starts by performing the derivation described in Section 2.3.2 for the lowest requested frequency. The λ_n value that is closest to zero at that frequency is labeled as Mode One. From there the next modes that have a λ_n value close to zero are labeled in ascending order. Calculations for the next frequency step then utilize CMA tracking algorithms to connect the similar current distributions between the two frequencies as a current distribution at one frequency may drop below another distribution in terms of significance at a different frequency (see [7] for more information on CMA tracking algorithms). It is difficult to ensure that all modes that have high significance over a given frequency range are

represented because a mode that is significant in a higher frequency may be behind many other modes in terms of significance at the lowest frequency.

A plot of the MS of the first three modes for the dipole is provided in Figure 14 and a graph of the current distributions of the first three modes is also provided in Figure 15. As shown in Figure 14, Mode One has a clear resonant behavior at 72 MHz. The wavelength that corresponds to that frequency is 4.16 m which is about twice the length of the dipole. This indicates that at that frequency the antenna operates as a half wavelength dipole antenna which has a current distribution that is consistent with current distribution (a) in Figure 15. There are similar expected consistencies with Mode Two's resonant frequency and its current distribution of a full wavelength dipole and Mode Three's resonant frequency and its current distribution of a 1.5 wavelength dipole. The characteristic current distributions are independent of a source which means that they are independent of an operating frequency. In other words, the weight of a combination of these modes (and an infinite number of higher order modes) is what changes based on the source and the modes themselves are characteristic of the antenna which is represented as

$$\frac{1}{|1 + j\lambda_n|}$$

from the derivation in Section 2.3.2.

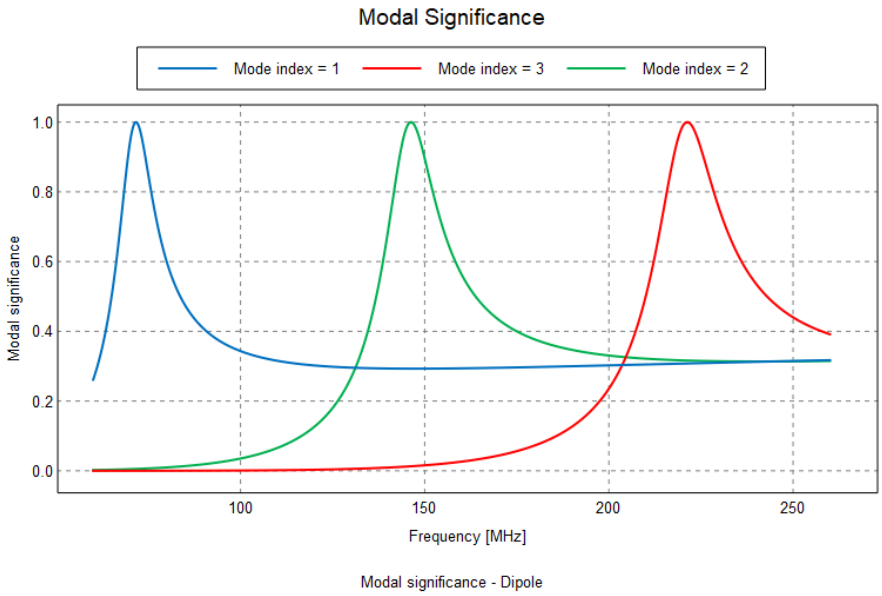

Figure 14: The MS plot of the first three modes of the center fed dipole antenna. A MS of one indicates that the current mode is resonant. Mode One is resonant at 72 MHz, Mode Two is resonant at 146 MHz and Mode Three is resonant at 220 MHz.

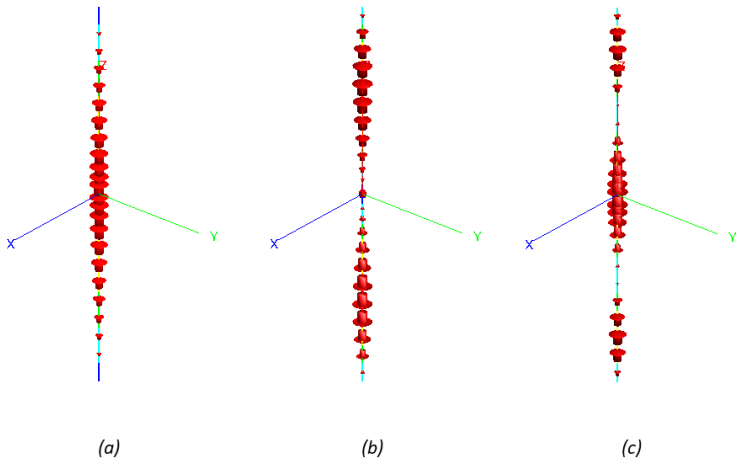

Figure 15: The first three characteristic current distributions solved with Feko. Modes 1-3 are displayed left to right from (a) to (c) respectively. The size of the arrows are used to display the relative magnitudes of the current. Peaks an nulls can be inferred and the overall wavelength of the each current is visualized along the antenna.

3.2.2 Modal Excitation Coefficient

The MEC is a measure of how well the excitation couples with each mode. It is represented in the derivation from Section 2.3.2 as $\langle J_n, E \rangle$ which is a mathematical way of describing how well the electric field from the source is aligned with the characteristic current. For this dipole example, the source was placed at the center of the antenna which creates the electric field that is used in the MEC calculation. Figure 16 shows the graph of the MECs for the first three modes of the dipole antenna which, at first, may seem unintuitive.

It is unexpected that Mode Three is the best at being the most coupled mode throughout the full observed frequency range, but consider the near-field electric field

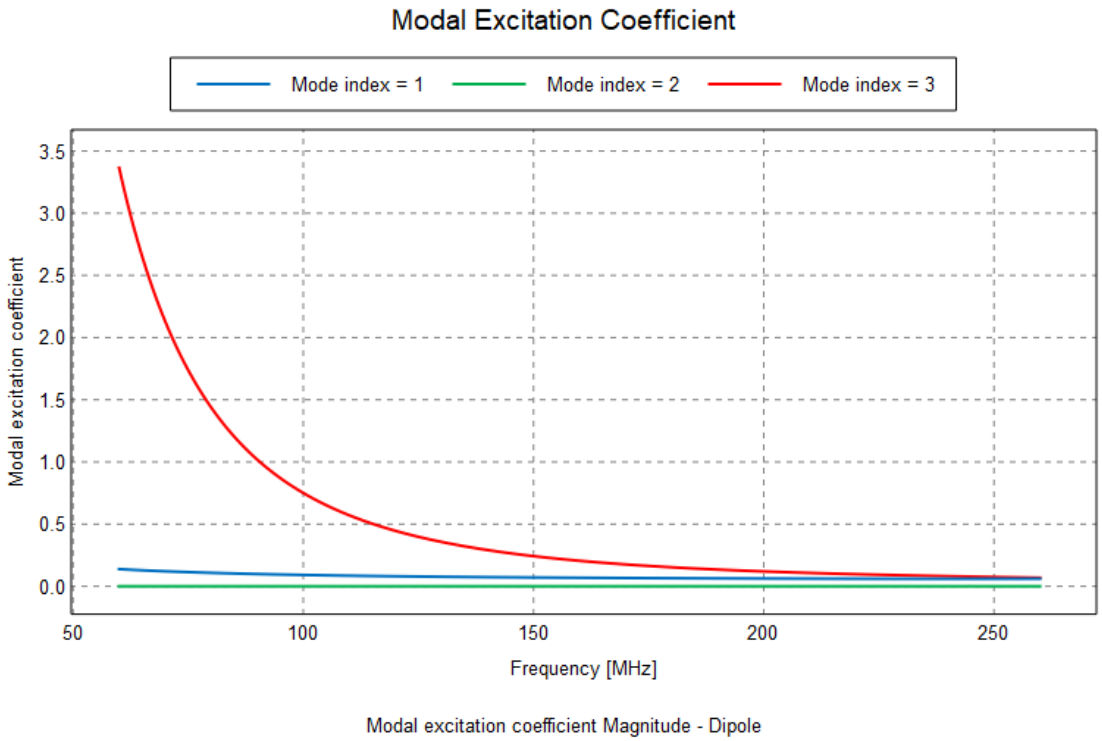

Figure 16: The first three MECs as a function of frequency solved with Feko. Mode 3 has a high MEC because the electric fields from the source are consistent with the current distribution at lower frequencies. Mode 2 is zero because the source for this antenna is placed at the null of mode 2's current distribution.

of the dipole shown visually and graphically in Figures 17 and 18 respectively at the three resonant frequencies. The peaks of the near-field line up with the peaks of Mode Three's current distribution, seen in Figure 15, more than the other modes. Mode Two is perfectly canceled out as the resulting inner product of J_2 and E always is zero. Generally, when the source is placed at the maximum of a current distribution, the MEC is greater and when the source is placed at a null, the MEC is nearly zero [7]. This guideline follows for Mode Two as the source is placed at a null and also follows for modes one and three where the source is placed at the peaks. Since the source is placed at the maximum of the current distributions for modes one and three, their MEC values are relatively higher than the other modes which will contribute to a greater MWC discussed in the next section. In summary, placement of the source drives the near field electric field which then is compared to each characteristic current distribution with the result being the MEC.

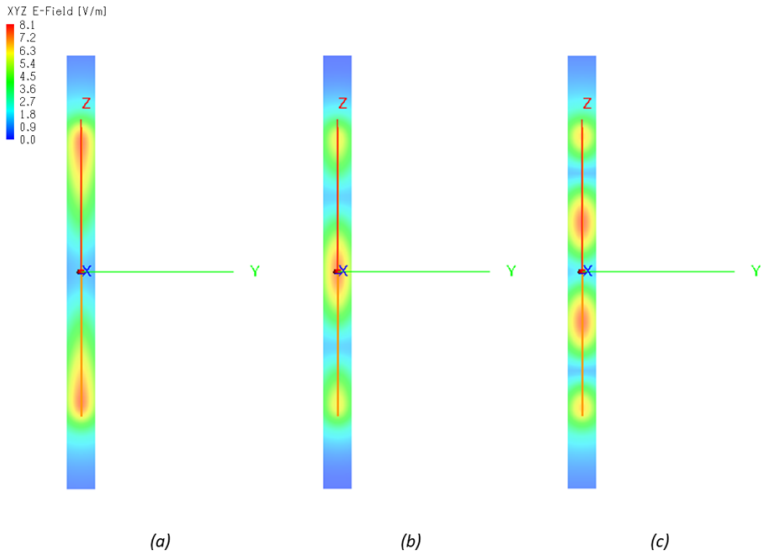

Figure 17: This is a visual of the relative peaks and nulls of the near field electric field for frequencies 72, 146 and 220 MHz. The relative maximums of the field are near the ends for 72 MHz which corresponds with Mode 3's current distribution seen in Figure 15. These fields with the current distributions create the MEC in Figure 16.

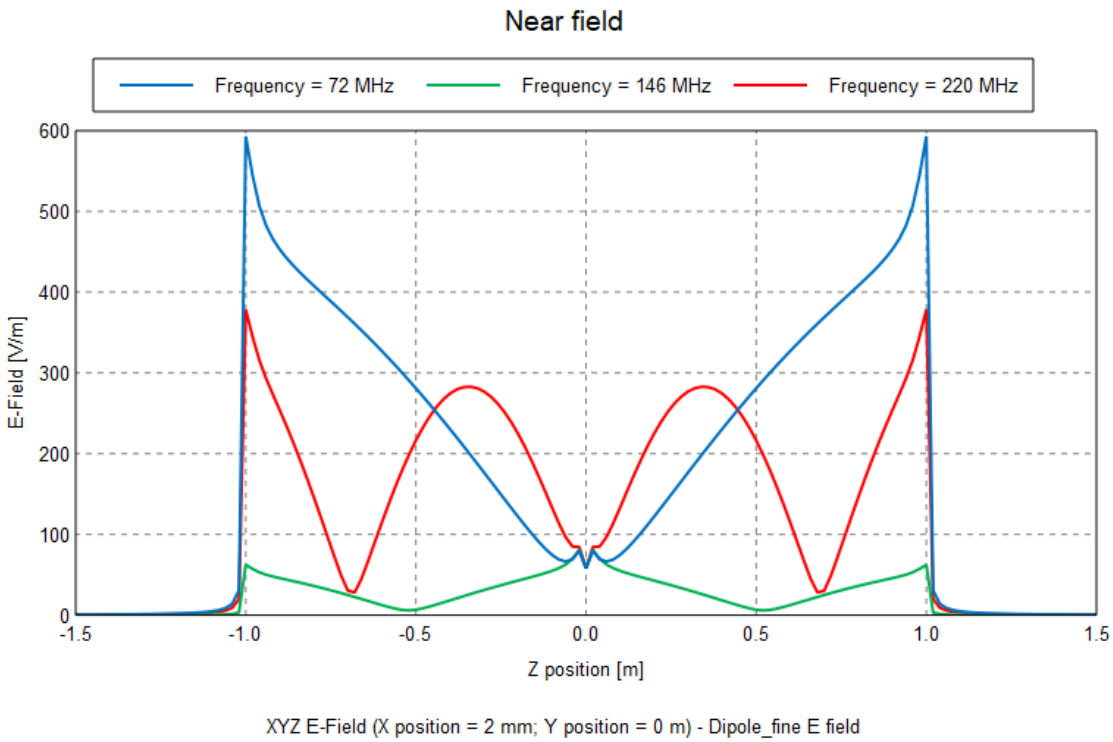

Figure 18: This is a graphical view of the near field electric field along the antenna body. The relative maximums are towards the ends of the dipole, especially for 72 MHz. This corresponds with mode 3's current distribution in Figure 15.

3.2.3 Modal Weighting Coefficient

The MWC is the product of the MS and the MEC for each mode. It represents how much each mode contributes to the observed current distribution at each operating frequency. Figure 19 shows a graph of the MWC of the dipole which reveals two frequencies where the MWC of one mode is substantially larger than the others. High MWCs correlate to frequencies that resonate with the antenna or, said another way, where the antenna impedance is nearly zero. Since the reflection coefficient is calculated based on the default assumption of a 50 Ohm transmission line, which is far closer to zero than the impedance of the antenna at any other frequencies, the antenna impedance seems to be matched well at the operating frequencies as shown

in Figure 13. However, it is worth stating that if the transmission line impedance was lowered to match the antenna impedance, the antenna performance would be even more efficient. Matching antenna impedance is a typical practice used in most applications.

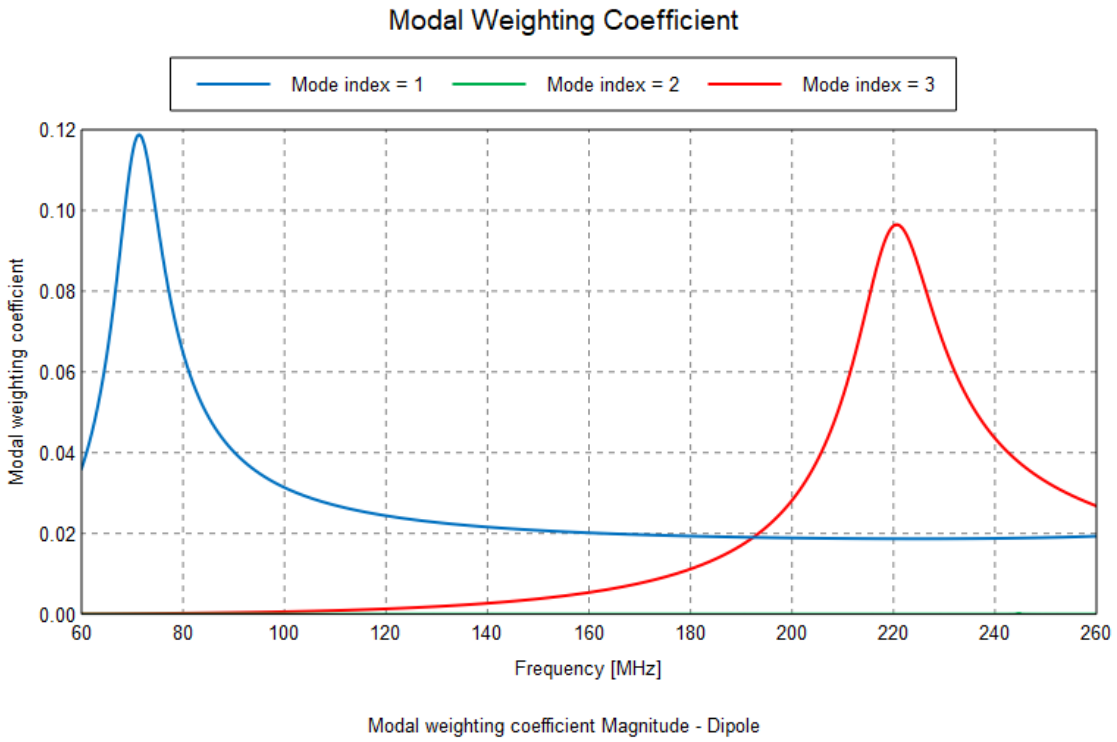

Figure 19: These traces are the first three MWCs as a function of frequency solved with Feko. Only modes 1 and 3 have significant values which corresponds with frequencies that this antenna will operate efficiently.

3.2.4 Design with Characteristic Modal Analysis

This center feed dipole example examines the performance of a known antenna as a way to demonstrate the underlying CMA and set a basis for how it can analyze results. However, for the purpose of being applicable to the main topic of this thesis, it is important to show how CMA can play a role in design decisions such as the feed placement rather than post design performance analysis. Antenna designers must

meet various requirements which in turn creates a wide variety of design procedures to which CMA can be used in different ways.

When the designer chooses a shape they will also be able to produce a graph of the MS of characteristic current distributions for a given frequency range. This can give the designer an idea of how easily current can be driven on the antenna to operate at a certain frequency. Conversely, if the shape is fixed but the operating frequency is free, a graph of the MS can give the designer an idea of a frequency that will resonate more easily for the antenna. If the shape and operating frequency are fixed, the MS in conjunction with the characteristic current distributions can be used to determine the optimal placement of the feed. This feed placement technique can also apply when treating the antenna mounting structure as an antenna and the actual antenna as the source as is examined in Section 3.4.

Revisiting the previous example but with an additional requirement of operating at 146 MHz, which it does not currently operate efficiently at as shown by Figure 13. If the new requirement was that the antenna only operated at 146 MHz, impedance matching using circuitry with a center fed dipole would be possible. However, this change creates new burdens on the design as the impedance of the antenna is much greater in magnitude and is complex. Impedance matching this way will usually only work for a single frequency and only for narrow band operation. A better design solution is to look at the graph of the MS (Figure 14) and see that Mode Two resonates at 146 MHz. Referencing the current distribution of Mode Two, seen in Figure 15, it seems a more optimal placement of the source would be 75% up the dipole. This source placement is not at the nulls of modes one or three (though not at the peak either so a small drop in performance is expected at those corresponding resonant frequencies), so it should still excite all three modes to a degree. The MECs and the MWCs of the new design are provided in Figures 20 and 21 respectively as well as

the overall reflection coefficient of the design in Figure 22. As expected, the MEC of modes one and three decreased and the MEC of Mode Two became non-zero. This, in turn, led to a peak in the MWC graph which corresponded to the graph of the reflection coefficient.

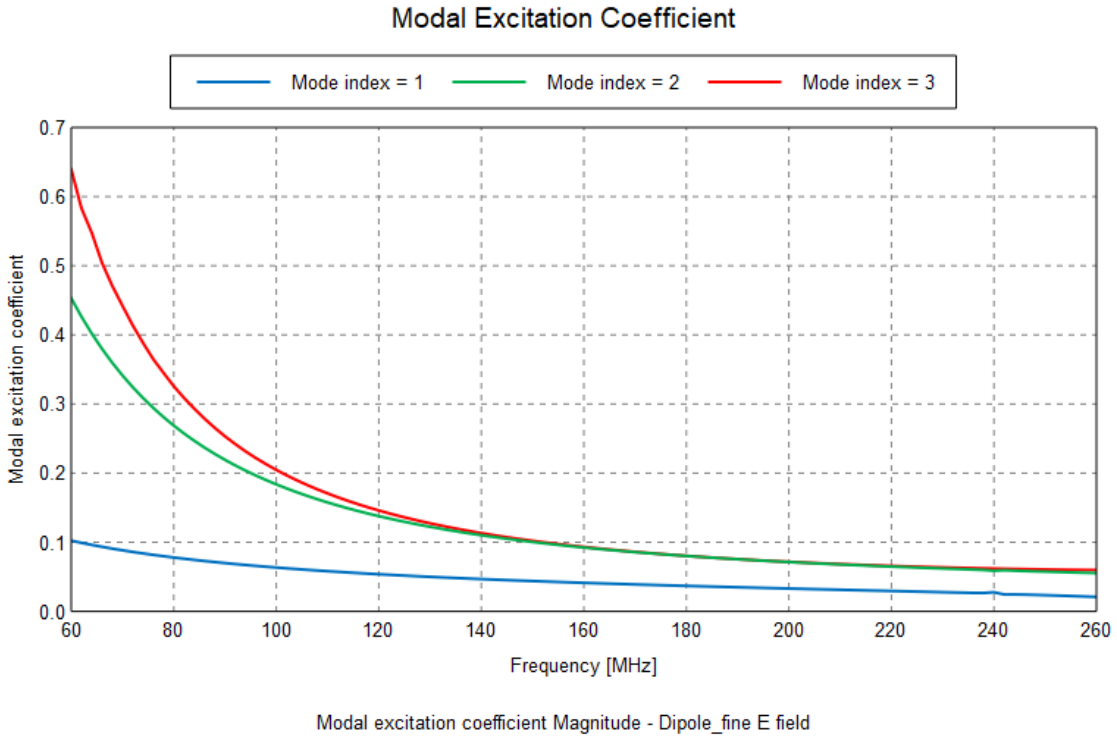

Figure 20: These are the first three MECs of the 75% fed dipole as a function of frequency solved with Feko. Mode 2 is adequately excited as opposed to the center fed dipole.

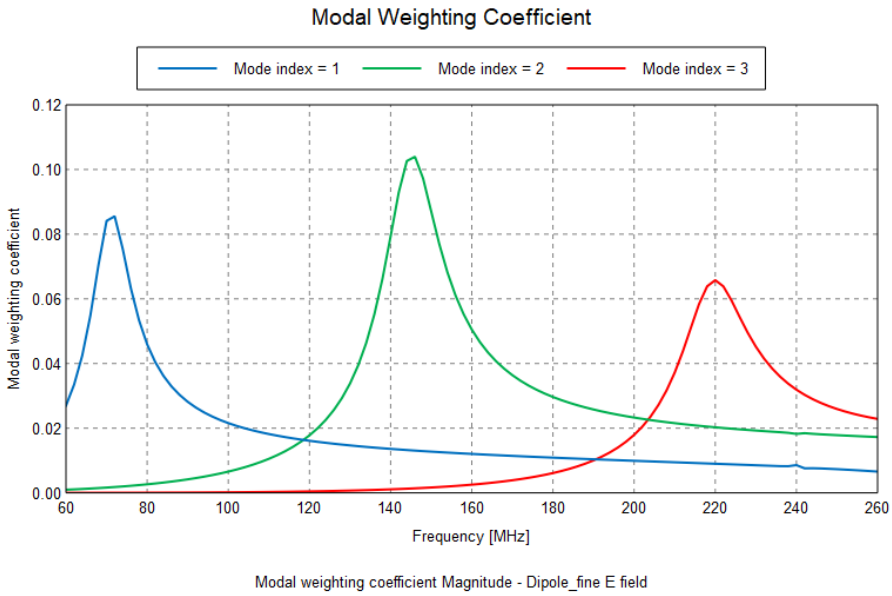

Figure 21: These are the first three MWC traces of the 75% fed dipole as a function of frequency solved with Feko. The significant values correspond to efficient antenna radiation.

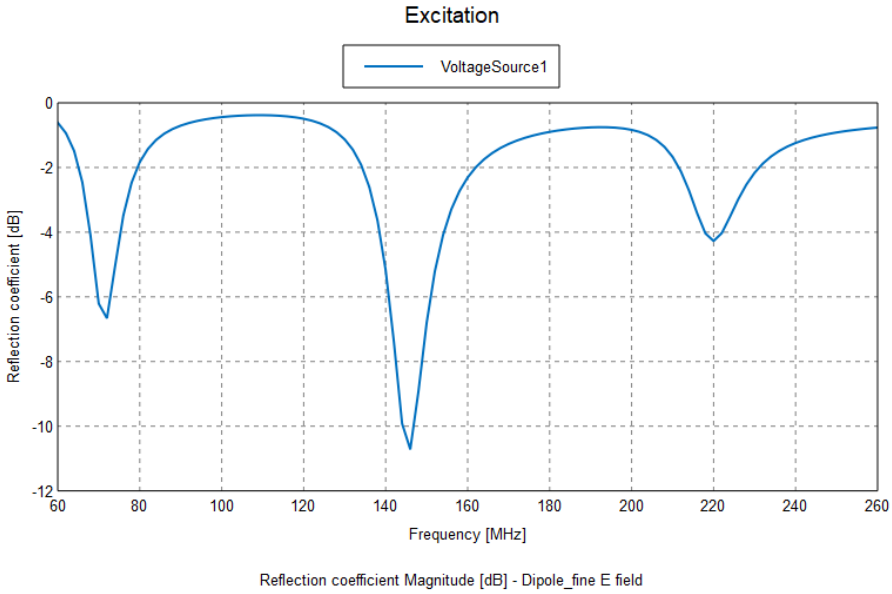

Figure 22: The reflection coefficient of the 75% fed dipole as a function of frequency solved with Feko. The objective of modifying the antenna to have an operating frequency at 146 MHz is shown.

3.2.5 Dipole Solution

The design requirements of the antenna application considered in this thesis, which include operating at 450 MHz and 2.285 GHz, can be met with a Dipole solution. The requirements can be obtained by first determining the length that will resonate well at the lower frequency. A 450 MHz operating goal corresponds with a half wavelength of about 33 cm. Performing CMA on a Dipole of that length and examining the higher operating frequency revealed a mode that is resonant at a frequency that is slightly lower than 2.285 GHz. Upon inspection of the current distribution of both modes that resonate at the target frequencies, the optimal fed location should be centered on the Dipole because both current distributions have a maximum at the center of the Dipole. Since the lower frequency resonates better than the higher frequency, the length of the Dipole can be optimized to bias toward the higher frequency and more evenly allow for equal performance at both operating frequencies. The result is a center fed antenna that has a length of 31.9 cm.

This thesis is focused on the theoretical design and operation of an antenna for a CubeSat but the optimal placement, integration, and deployment of the antenna with regards to the CubeSat is not in the scope. However, to demonstrate the viability of the Dipole design, a basic Perfect Electrical Conductor (PEC) model of the CubeSat with the antenna is simulated. The Dipole conveniently fits in between the solar panels as a possible area for deployment. Figure 23 will show the configuration and Figure 24 will show the relative gain in the assumed nadir-pointing direction. The polarization of the radiation is not circular so it will partially degrade in the ionosphere but is still a strong signal. Although there are many other metrics that can be analyzed from the design, Figure 24 proves that the design has met the minimum operating requirements.

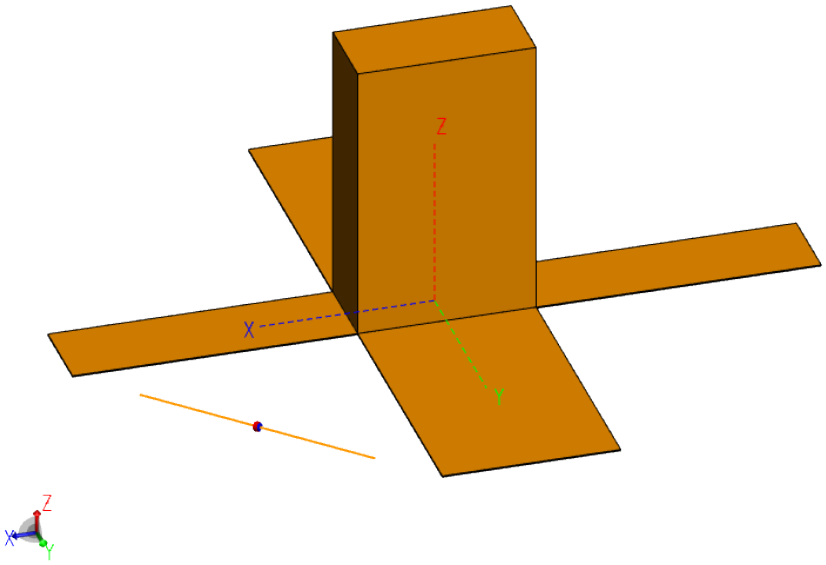

Figure 23: This figure shows the proposed configuration/orientation of a 31.9 cm Dipole antenna with regards to the satellite body.

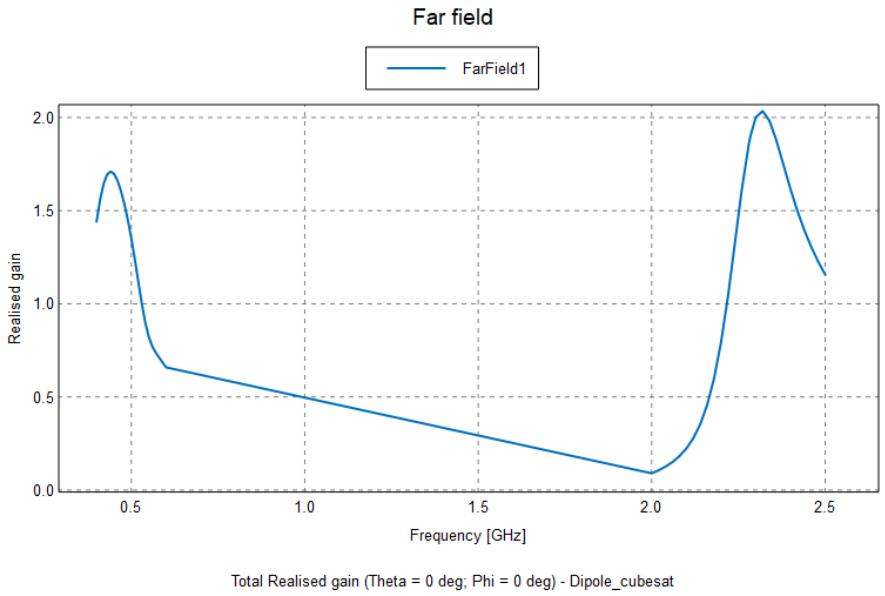

Figure 24: This plot shows the realized gain as a function of frequency for operation. There are two clear operating frequencies at 450 MHz and 2.285 GHz as intended.

3.3 The Metasurface Application

Metasurface antenna design also have been shown to utilize CMA in recent research. The current distributions along a metasurface are complex but with CMA the dominate modes become clear and explain the operation. However, initially designing a metasurface takes experience. Many designers often start with a certain pattern and shape that are spaced a certain way. This thesis does not start with a pre-existing metasurface but shows how CMA can guide the design itself to promote the desired mode and suppress undesired modes. This method of analysis has also been shown to be useful in tailoring an antenna's polarization by using Characteristic Angles derived from the CMA. Before CMA can be applied, a base antenna needs to already exist which has its own design choices to consider. Once the base antenna is conceived, CMA can be applied at both target frequencies to gain insights into a metasurface design that improves the antenna's performance. Finally, the theorized antenna can be simulated with the CubeSat structure to verify the desired performance.

3.3.1 Base Patch Antenna Design

Patch antennas are often desirable because of their incredibly low profile. For a CubeSat application, this quality is especially important as space and weight can be extremely costly. For these reasons a large amount of research has gone into patch antenna design and creation. Refer to Section 2.1 for a brief explanation on how patch antennas work and the different design trade offs that must be considered.

For the antenna needed in this thesis, an aperture coupled feed was chosen because the aperture and patch can work together in more complex ways to allow for operation at multiple frequencies. These complexities make the antenna harder to analyze and the results from CMA less insightful. Additionally, a size restriction of 10 cm X 10 cm will also be imposed. This makes operations at the lower frequency target difficult,

as the half wavelength (which generally drives the size of the antenna) is 33 cm. Adjusting the height and relative permittivity of the dielectrics can compensate for the smaller size and adjusting the aperture dimensions can maintain good operation at the higher frequency target as well. FEKO's optimization features were also used to fine tune the dimensions of the microstrip which drives the electric field. All factors used to design the base antenna are shown in Figure 25, of which the dimensions and breakdown are shown in Figure 26 and Table 1.

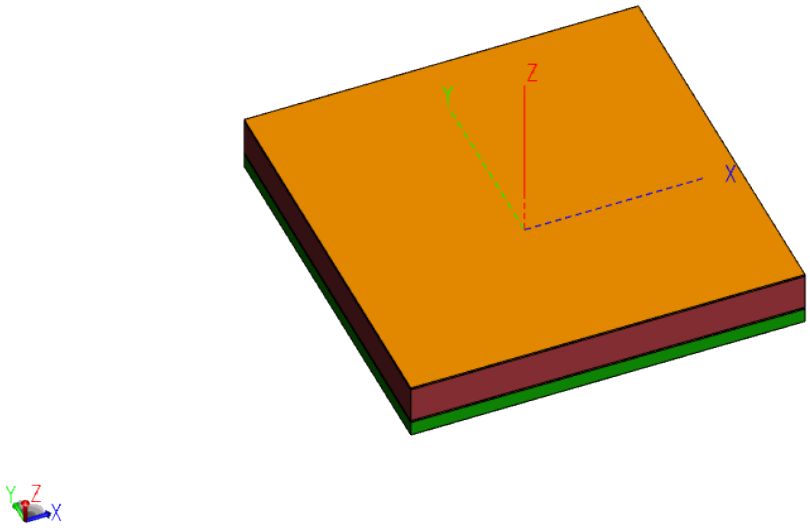

Figure 25: This is a visual model of the Base Patch Antenna design which is first analyzed.

The performance of this base patch antenna is surprisingly already close to the desired performance without need for a special metasurface to refine its operation. A graph of the realized gain is shown in Figure 27 for the low frequency band and Figure 27 for the high frequency band. Both figures show good operation at both target frequencies.

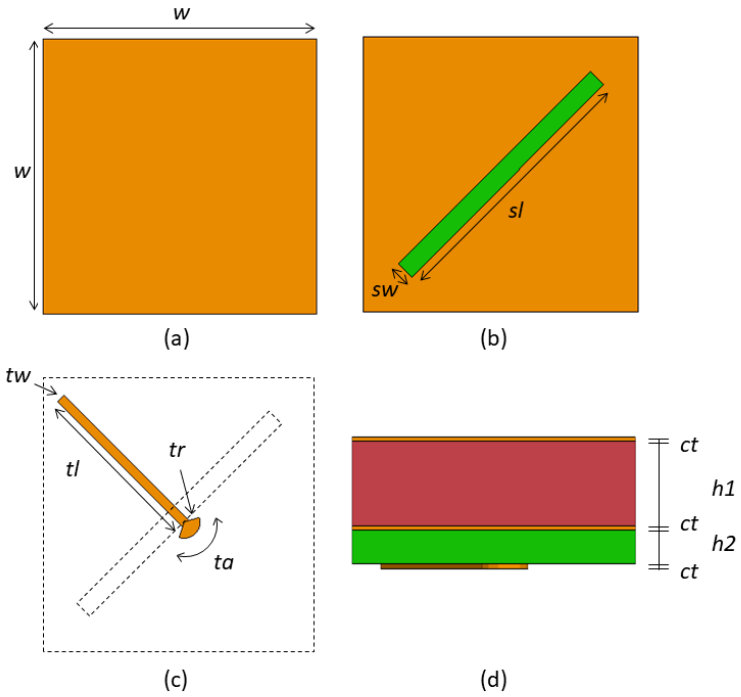

Figure 26: These are the layers of the Base Patch Antenna design. Sub-figure (a) shows the patch layer on top, sub-figure (b) shows the ground plane with the aperture cut out, sub-figure (c) shows the transmission line feed strip layer on the bottom, and sub-figure (d) provides a profile view.

Table 1: Base Patch Antenna Breakdown

Description	**Variable**	**Value (m)**
Patch Width	w	0.100
Slot Length	sl	0.025
Slot Width	sw	0.007
Transmission Line Length	tl	0.058
Transmission Line Width	tw	0.003
Transmission Line Radius	tr	0.010
Transmission Line Angle	ta	175.572°
Copper Thickness	ct	0.001
Dielectric 1	h_1	0.010
	ϵ_r	11.700
Dielectric 2	h_2	0.004
	ϵ_r	11.200

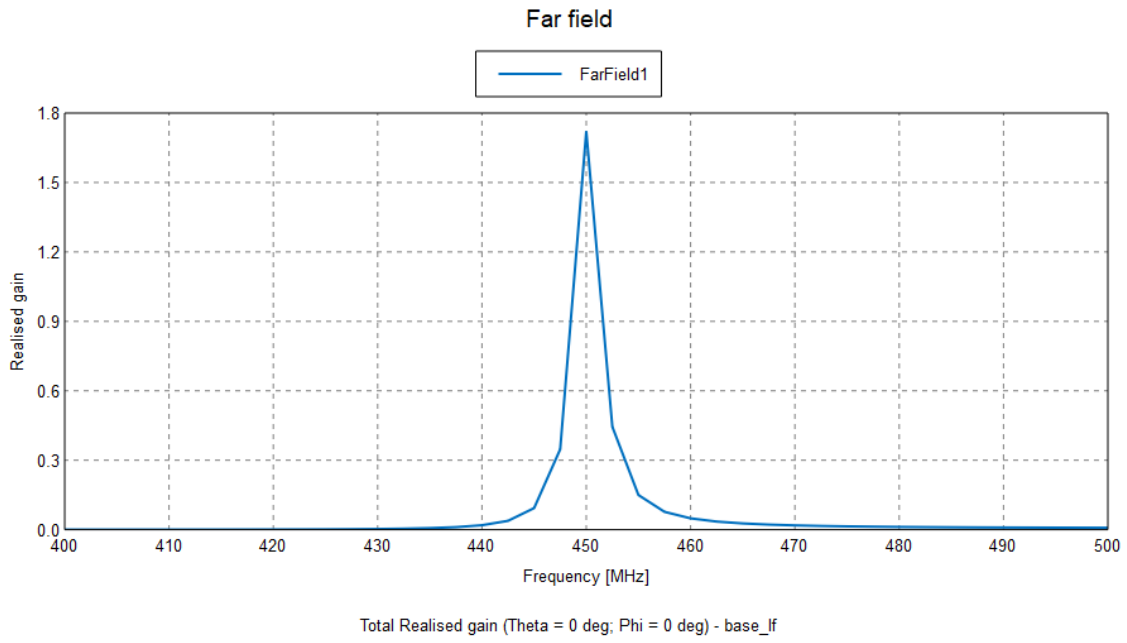

Figure 27: The Base Patch Antenna realized gain at the low frequency band. There is a larger realized gain at the target low frequency. Although the bandwidth is narrow, the requirement only needs a bandwidth of .5 MHz.

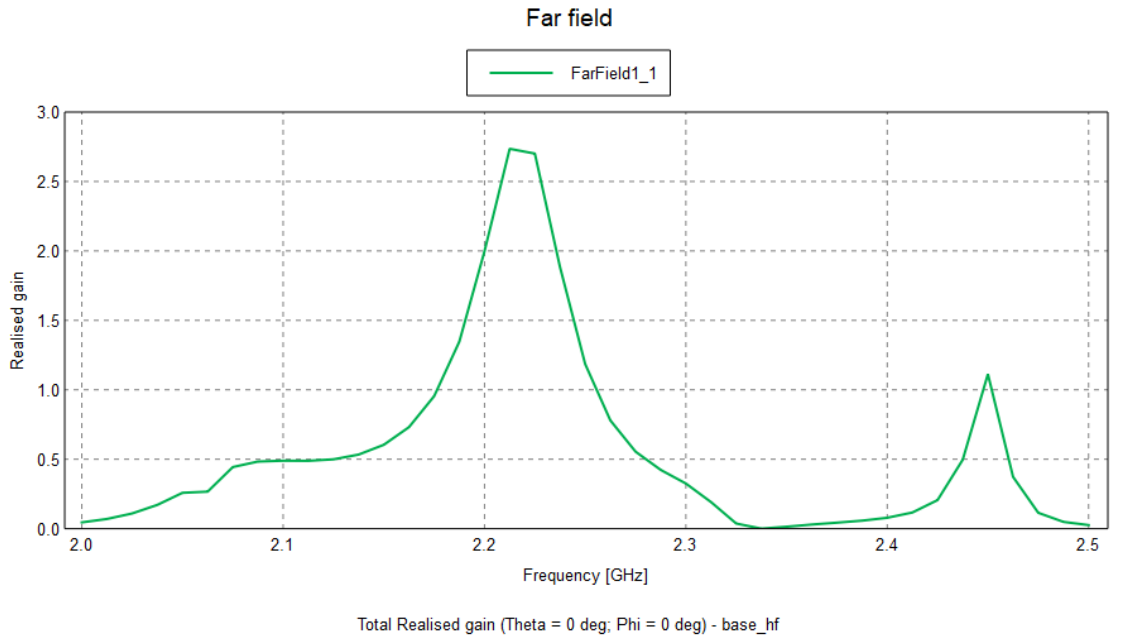

Figure 28: The Base Patch Antenna realized gain at the high frequency band. This graph indicates a high realized gain at the second target frequency

3.3.2 Characteristic Modal Analysis for Metasurface Antenna

Now that an antenna structure has been modeled, the structure can be put through the CMA process. First the lower target frequency is examined. This antenna size is already electrically smaller than most antennas, therefore special design changes like the feed structure and dielectric have already been made. It is for these reasons that there are only two symmetric modes that have any significant MS (see Figure 29). The current distribution of these modes go along the longest dimension (the diagonal) of the patch as shown in Figure 30. In other words, this mode is the only mode that resonates at 450 MHz that the patch antenna structure can support. The other less significant mode that goes along the opposite diagonal also has a stronger MS, but it has a near zero MEC because it does not align with the underlying microstrip's orientation. However, the microstrip is oriented so that it successfully excites the desired mode and a significant MEC/MWC is produced at 450 MHz. This then corresponds to the good operation and relatively high value of the realized gain at that frequency as shown in the graph in the previous section, Figure 27.

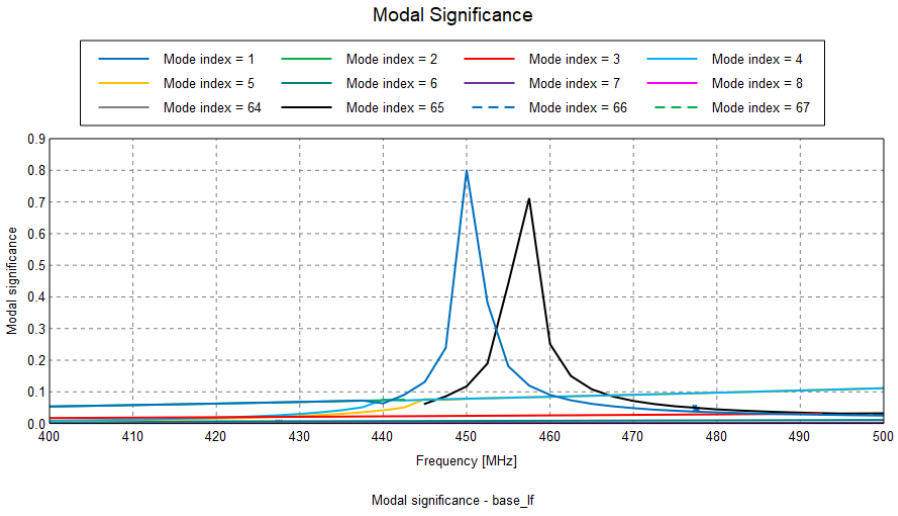

Figure 29: The Base Patch Antenna MS at the low frequency band. This plot identifies the only two modes with any significance at the target frequency.

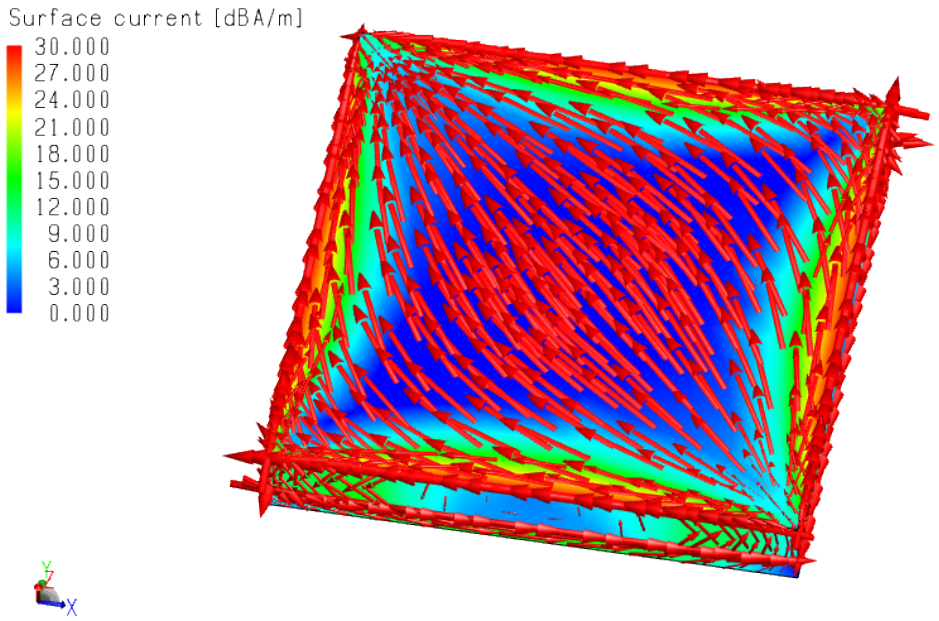

Figure 30: This is the Base Patch Antenna current distribution of Mode One; the most significant mode at the target low frequency. The current is oriented along the diagonal because it is the longest dimension and this antenna is electrically small for the given frequency.

The antenna is electrically small for the lower frequency band but is electrically large for the high frequency band. A small electrical size limits the number of characteristic mode whereas a large size introduces a large number of complex modes. These complex modes are difficult to isolate and excite with a simple source. The current distribution of the mode with the highest MWC at the target frequency is shown in Figure 31, and Figure 32 shows a graph of the MWCs of some of the modes that exist. This demonstrates that the antenna will operate with high-order multimodal currents. These modes are three dimensional and there exist complicated currents within the dielectric as well as the current on the surface. Even though the distribution is complex there is one useful thing that can be observed. This distribution is strong along the diagonal which is why it was, at a minimum, more efficiently excited due to its orientation.

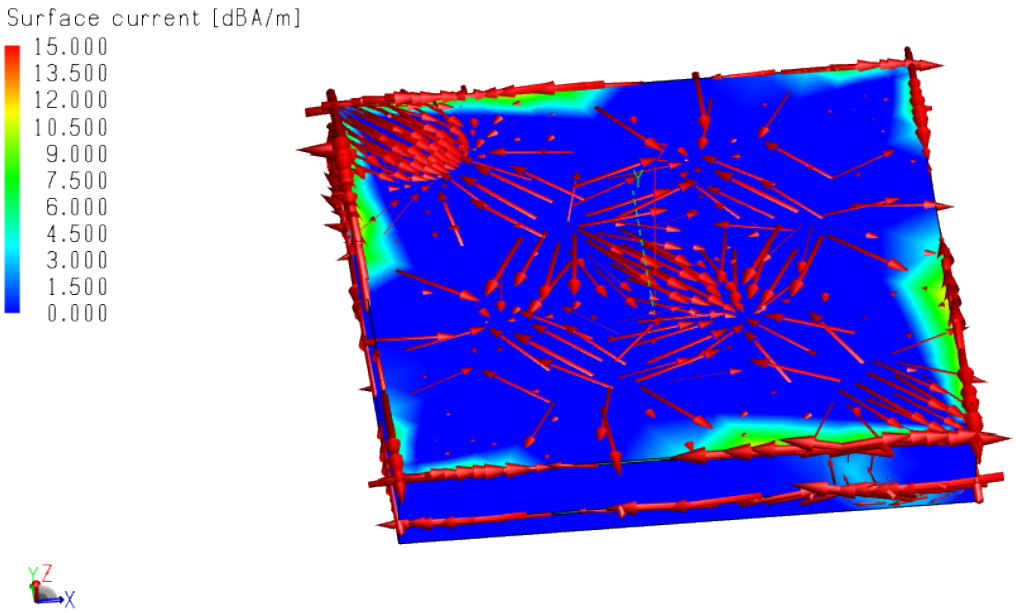

Figure 31: This is the Base Patch Antenna current distribution of the significant mode at the target high frequency. It is complex but still has a trend along the diagonal that the microstrip underneath is oriented.

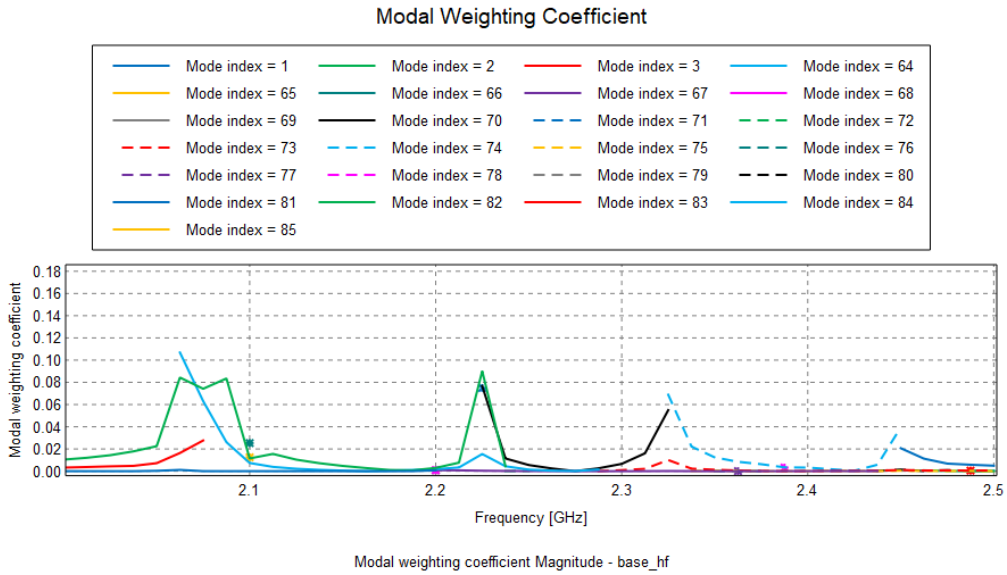

Figure 32: This is a plot of the Base Patch Antenna MWC for different modes at the target high frequency. The fact that there are so many indicates that it uses high order multi-modal operation at these frequencies.

The explanations above show that CMA, while useful in the operation of the antenna, can not offer much for design in this scenario. However, a few design changes regarding the metasurface can still be considered using CMA. Creating cuts in the surface along a desired mode's current distribution will not impede the current distribution and can be used to suppress undesired modes. For this application, the current distributions at both target frequencies are strongly aligned with the diagonal of the patch. When a cut along that diagonal is introduced, the operation of the antenna is nearly unchanged. This cut normally would suppress any other significant excited modes that did not align, but in this example these are the only two modes that are significant and excited. To further prove this assertion, another metasurface is analyzed that has cuts which follow the lower frequency current distribution but not the higher frequency. Unsurprisingly, this design still resonates at 450 MHz but no longer operates well at 2.285 GHz. Figure 33 shows all the described metasurfaces and Figures 34, 35, and 36 show their corresponding performance.

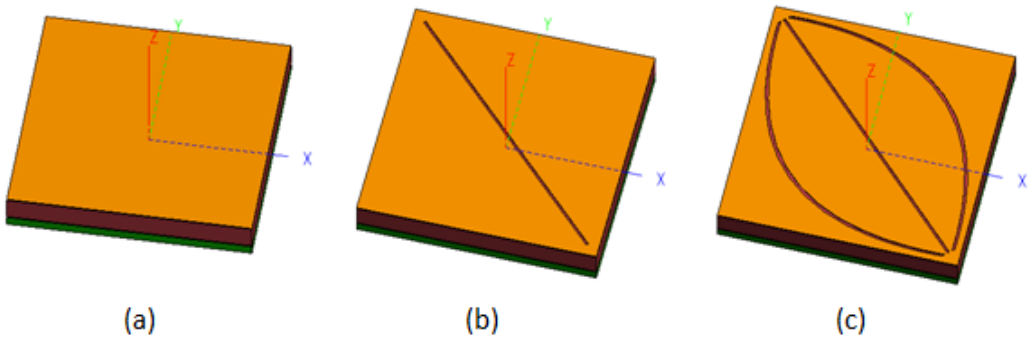

Figure 33: This figure shows the three metasurfaces that are analyzed. Sub-figure (a) is the Base Patch Antenna, it does not have any cuts. Sub-figure (b) is the first metasurface with a cut down the diagonal. Sub-figure (c) is the second metasurface with curved cuts that conform to the lower target frequency current distribution but not the higher target frequency.

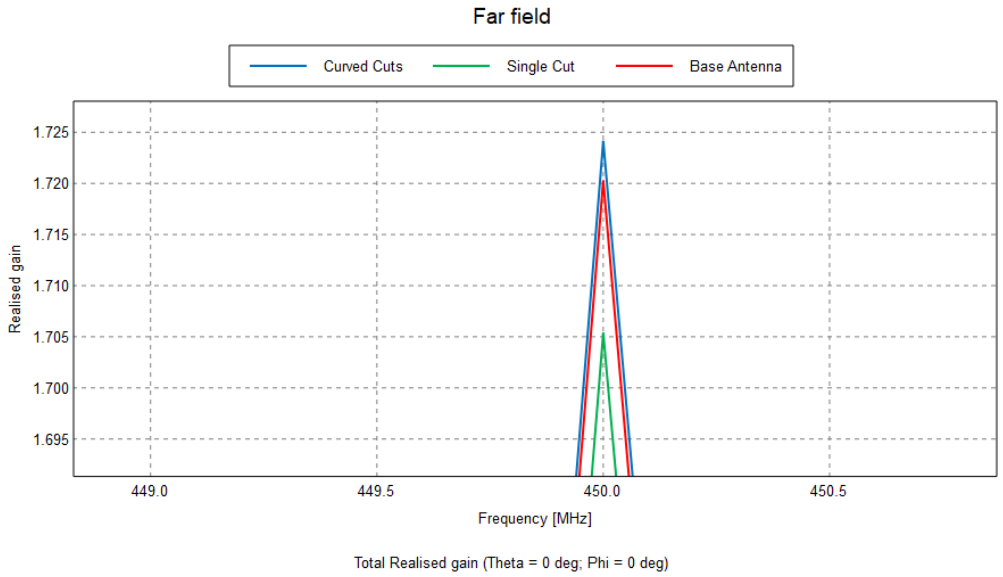

Figure 34: A zoomed in graph of the realized gain at the low target frequency. This shows that even though they are distinct, the performance of each design is barely different in performance.

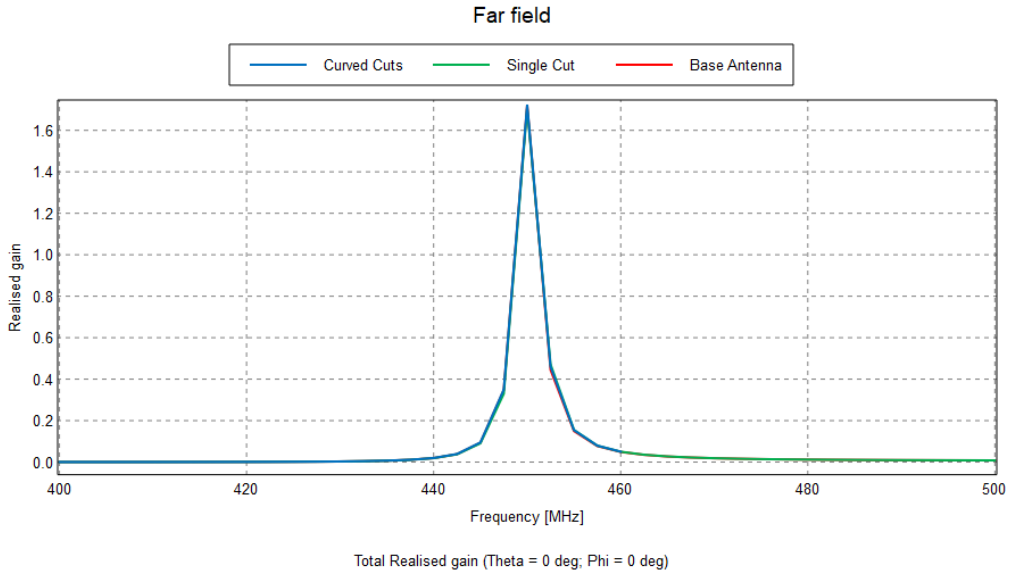

Figure 35: This is a graph of the realized gain at the low target frequency for the three different antenna designs. The performance of each design is barely different in performance.

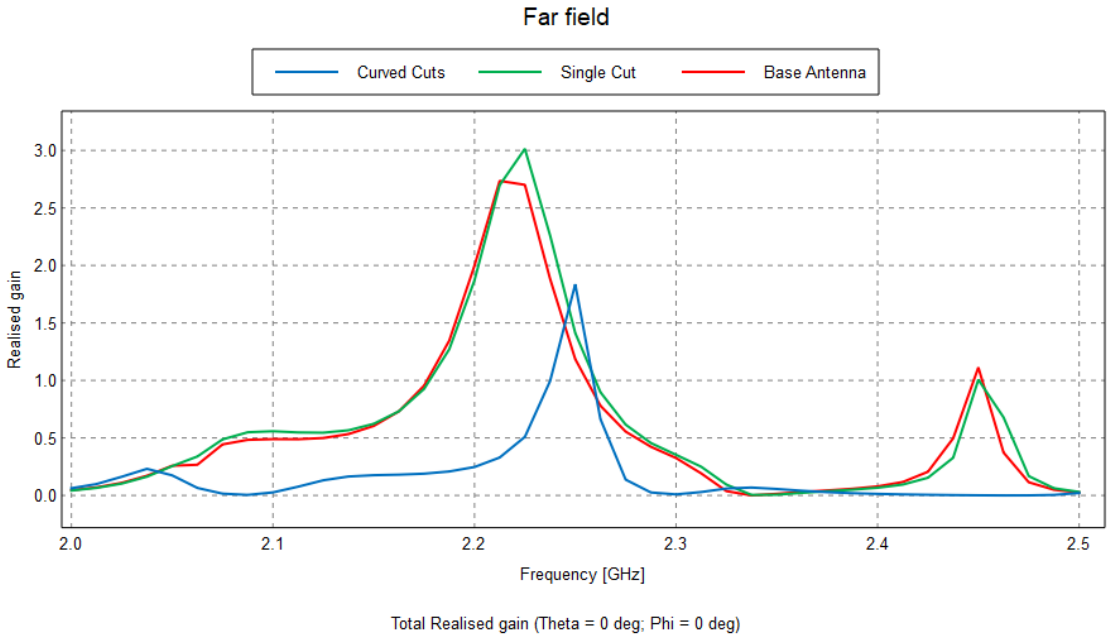

Figure 36: This is a graph of the realized gain at the high frequency band. The design with a cut that is consistent with the dominant mode has nearly the same performance as the original design. The third design with curved cuts clearly has worse performance at the target frequency.

3.3.3 Full Model Simulation

To be thorough, an analysis of the patch antenna mounted to the CubeSat should be done to verify that the operation of the antenna is not too adversely affected by the surrounding structure. Another change that has not been simulated so far is that the ground plane will be replaced with the CubeSat structure itself. This will change the shape of the ground plane. A model of integrated antenna is shown below in Figure 37 and Figure 38 is a plot of the realized gain of the model over the frequency bands of interest.

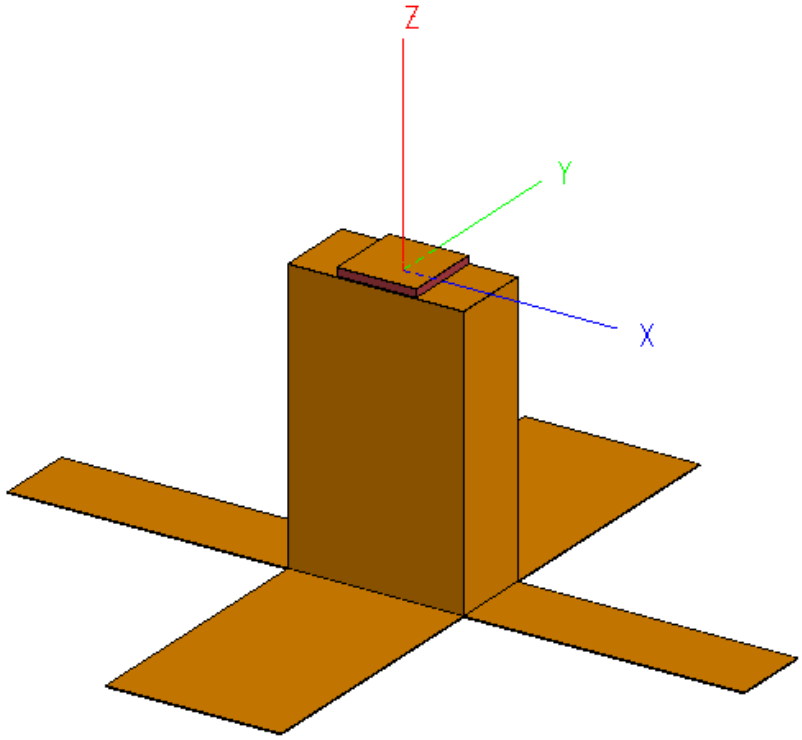

Figure 37: This is a figure of the patch antenna integrated into the CubeSat structure.

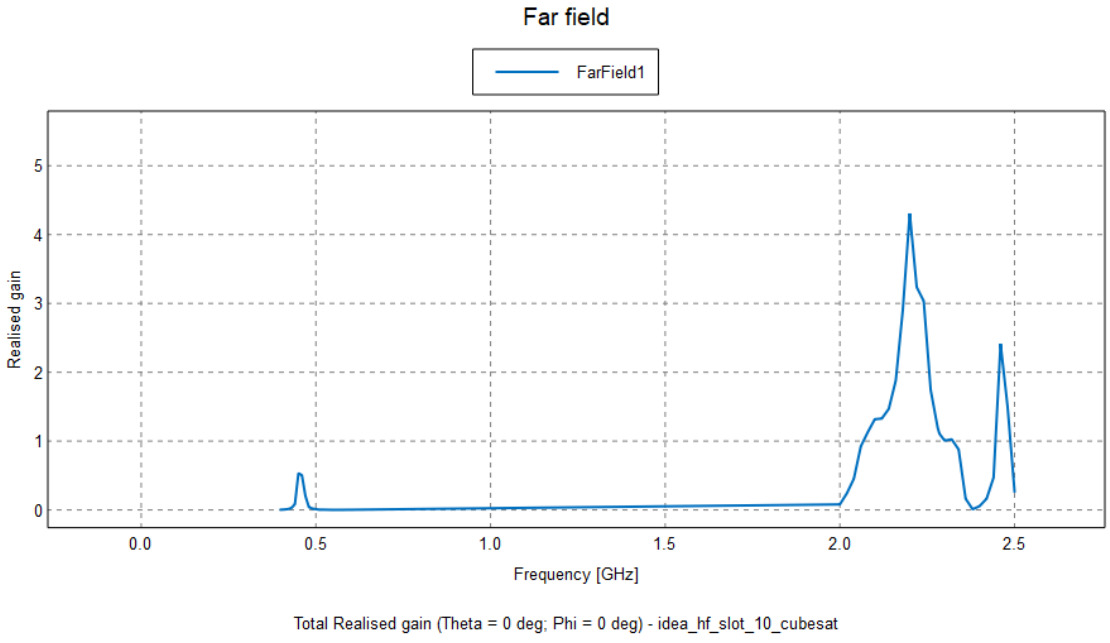

Figure 38: A graph of the realized gain of the patch antenna integrated into the CubeSat structure. It show that the satellite structure biases operation towards the higher frequency when compared to Figure 27.

3.4 The Chassis Radiation Application

Usually an antenna size is on the order of the wavelength they are designed to operate. There are ways to modify the electrical size required of an antenna by using clever shapes or high permittivity dielectric materials, but generally it can be quite difficult to operate at a frequency that has a wavelength much greater than the antenna body. Depending on the application it may be possible to utilize a surrounding structure that is on the order of the desired wavelength to excite a current distribution which produces the desired radiation. The problem then becomes what kind of current distribution produces the desired effects and how is that distribution optimally excited. These questions can be answered using CMA. For this thesis's application, the operating frequency of 450 MHz has a wavelength of about 66 cm and the higher frequency 2.285 GHz has a wavelength of about 13 cm. The dimensions of the CubeSat with deployed solar panels is about 92 cm by 81 cm by 35 cm. While the dimensions do not exactly equal the wavelength of the lower frequency, they are on order with it so it is possible for the CubeSat structure to act as an antenna. This reduces the design challenge to an antenna that only needs to operate at the target high frequency but also properly excites the CubeSat structure. The analysis performed in thesis uses a simplified smooth uniform PEC model of the AFIT CubeSat structure which should be redone more accurately if this application is being considered practically.

3.4.1 Characteristic Modal Analysis of Satellite Structure

No source is required to calculate the MS of a structure. Figure 39 shows the MS of modes that resonant near 450 MHz. Although the figure does not show any modes at the target frequency, there are still four modes which have a relatively high MS. Modes one and two have a current distribution, shown in Figures 40 and 41, which

resemble a dipole in which current is mostly flowing along the long edge on the solar panels. The resonant frequencies of 170 MHz for modes one and two is consistent with the length of the solar panels being about .92 m. Mode nine also has a high MS at 450 MHz. However, its current distributions, shown in Figure 42, is a bit harder to analyze and a bit more complex, yet still has relative maximums on the edges of the solar panels.

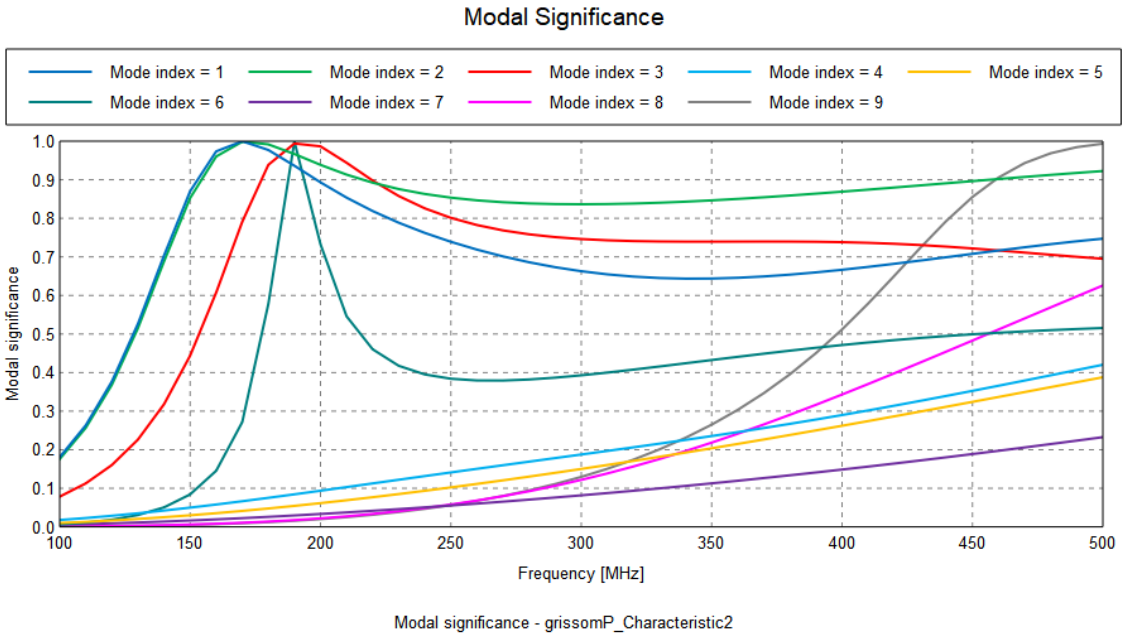

Figure 39: This graph shows the MS of modes at the low frequency band. Some of the traces are resonant near 170 MHz because that corresponds to the full length of the satellite with the deployed solar panels. This plot is needed to identify which modes will have a high MS at the target frequency.

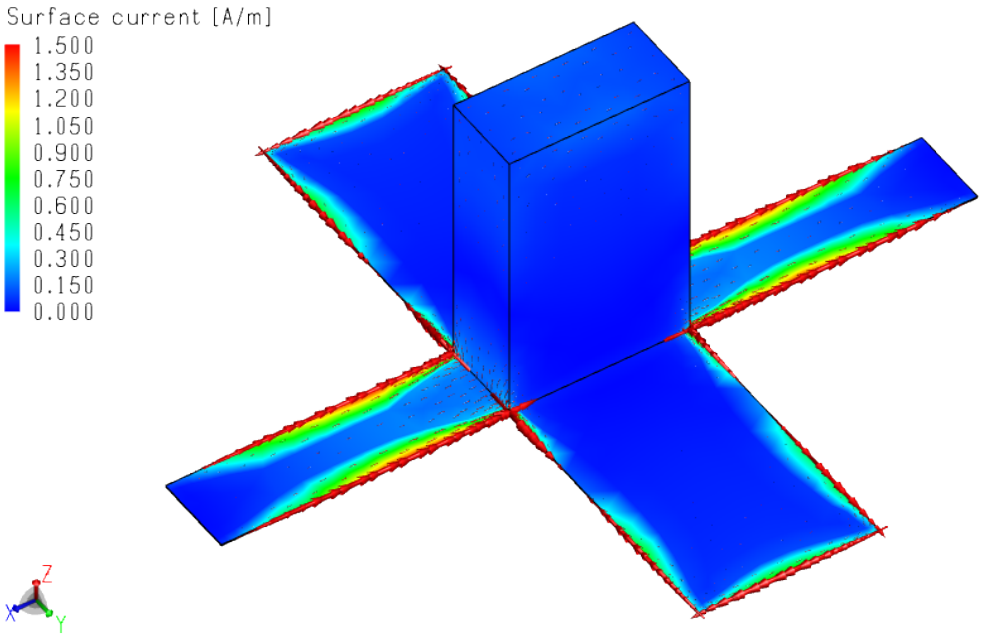

Figure 40: This is the current distribution of Mode One at the low target frequency of 450 MHz. It has relative maximums on the edge of the skinny solar panels.

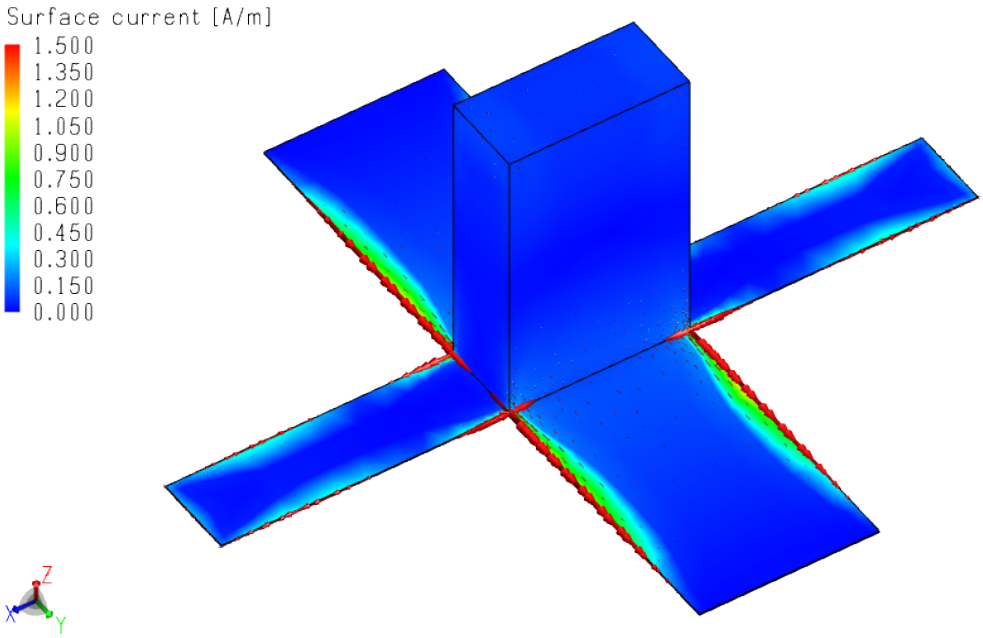

Figure 41: This is the current distribution of Mode Two at the low target frequency of 450 MHz. It has relative maximums on the edge of the skinny solar panels.

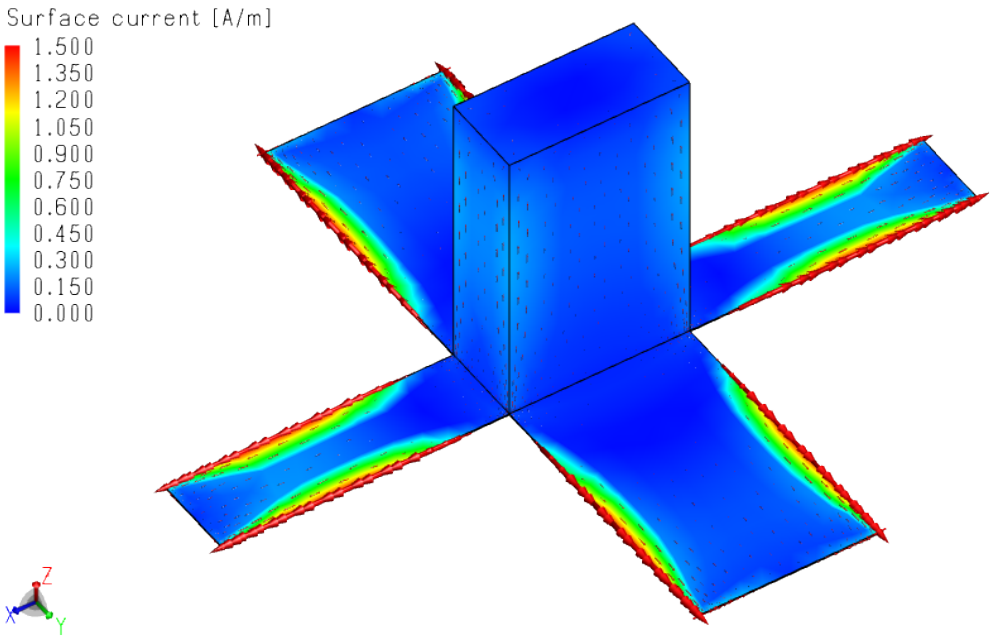

Figure 42: This is the current distribution of Mode One at the low target frequency of 450 MHz. It has relative maximums on all edges of the solar panels.

Modes one and two are relatively simple, mostly symmetric, and high in MS, so it makes sense to choose them as the modes to attempt to excite. The next step is to design an antenna that will cause a high MEC, which is calculated by $\langle J_n, E \rangle$ from Section 2.3.2. This means that the antenna needs to be designed to have a near-field electric field that efficiently excites the predicted current distribution, especially at the peaks of the current distribution.

3.4.2 High Frequency Antenna

By using the CubeSat structure to radiate efficiently at the lower frequency, the operation at the lower frequency requirement has been traded for an electric near-field requirement. Simple antennas like a dipole or loop antenna operate well at the high frequency but do not additionally produce a strong enough electric field at the lower frequencies. A patch antenna with an aperture coupled feed produces strong fields

at low frequencies by radiating off the feed and still radiates off the patch for higher frequencies well.

The majority of the design has already been performed in the previous section, The Metasurface Application, Section 3.3. However there are a few deviations as the requirements are slightly different. There still are three conductive layers; the transmission strip line, the ground/slot layer, and the patch layer. For this model, the real life dielectric material gallium arsenide will fill the space between the layers. Gallium arsenide is commonly used in manufacturing electronics because of its relatively high relative permittivity which, for this application, can increase the electrical size of radiating elements. This allows the patch to be designed in a more compact fashion staying within a size of 10 cm x 10 cm x 20 mm. A simulated source was introduced between the end of the transmission strip and the ground plane. The dimensions of the design are shown in Table 2 and Figure 43.

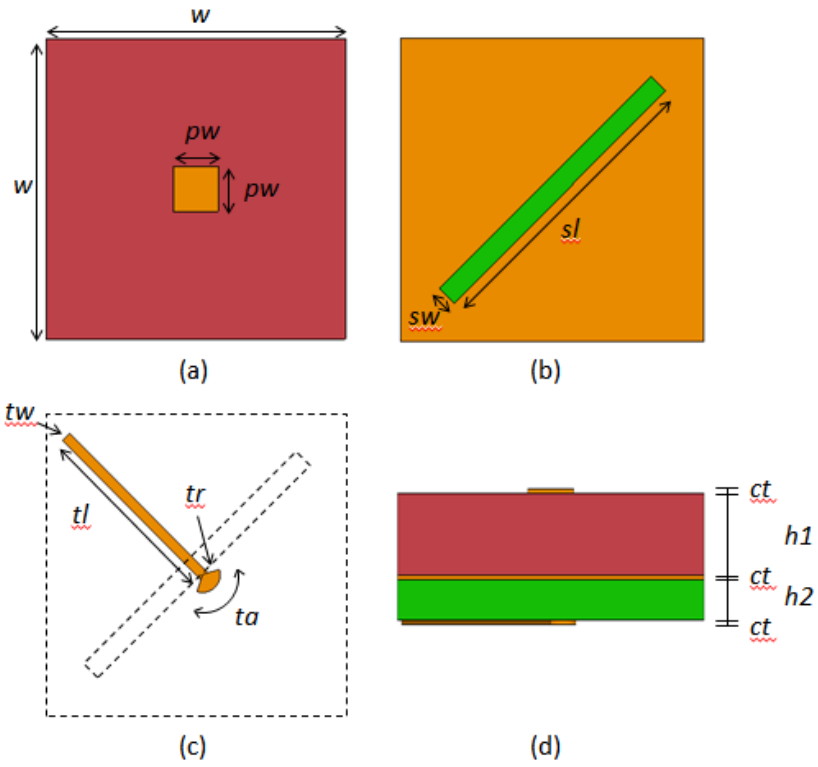

Figure 43: These are the layers of the high frequency antenna design. Sub-figure (a) is the patch layer on top and it is smaller than the patch in the Metasurface Application because it is made to optimize only the higher frequency target. Sub-figure (b) is the ground plane with the aperture cut out, sub-figure (c) is the transmission line feed strip layer on the bottom, and sub-figure (d) is a profile view.

Table 2: High Frequency Patch Antenna Breakdown

Description	**Variable**	**Value (m)**
Width	w	0.100
Patch Width	pw	0.015
Slot Length	sl	0.099
Slot Width	sw	0.007
Transmission Line Length	tl	0.070
Transmission Line Width	tw	0.004
Transmission Line Radius	tr	0.006
Transmission Line Angle	ta	125.350°
Copper Thickness	ct	5E-4
Dielectric 1 (GaAs)	h_1	0.010
	ϵ_r	12.900
Dielectric 2 (GaAs)	h_2	0.005
	ϵ_r	12.900

Patch antennas generally have a main lobe of radiation directly perpendicular to the patch and this particular antenna is no exception. Figure 44 shows the realized gain looking directly at the patch, which demonstrates that the design efficiently radiates at the target frequency of 2.285 GHz. The reflection coefficient of the antenna can also be used to assess the design and also supports its operation at 2.285 GHz. Figure 45 shows the reflection coefficient and reveals an inefficient and inoperable behavior at the lower target frequency of 450 MHz. However, Figure 46 reveals that the near fields at that frequency are not negligible which is leveraged with the satellite's chassis.

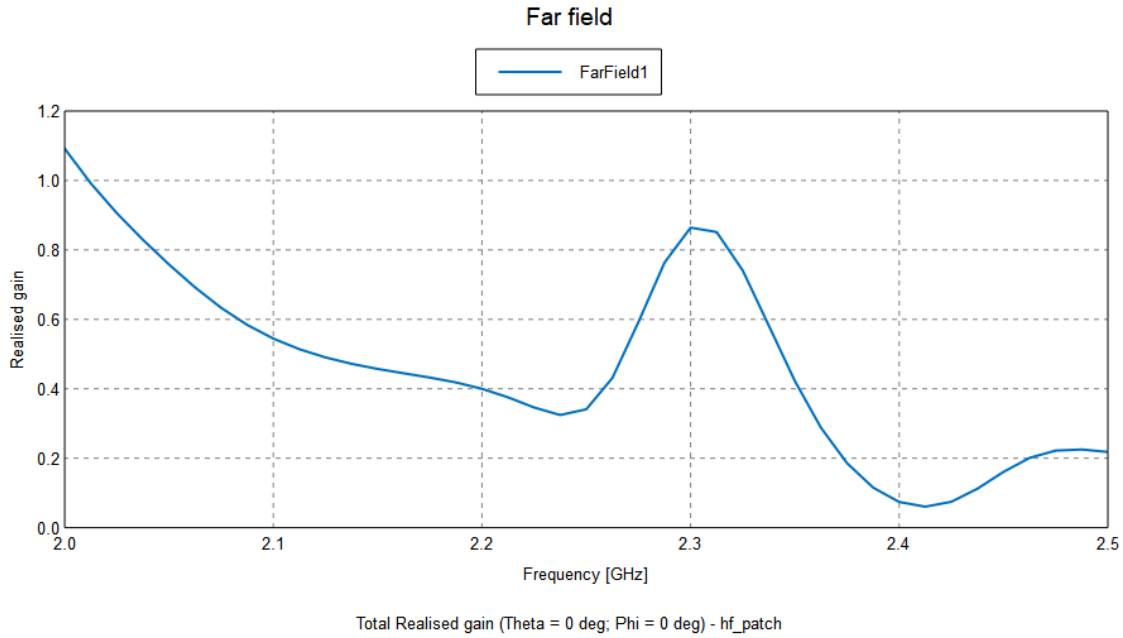

Figure 44: This is a plot of the realized gain at the high frequency band for the antenna designed to operate at the high frequency target. It shows a relative maximum at the target frequency implying efficient operation.

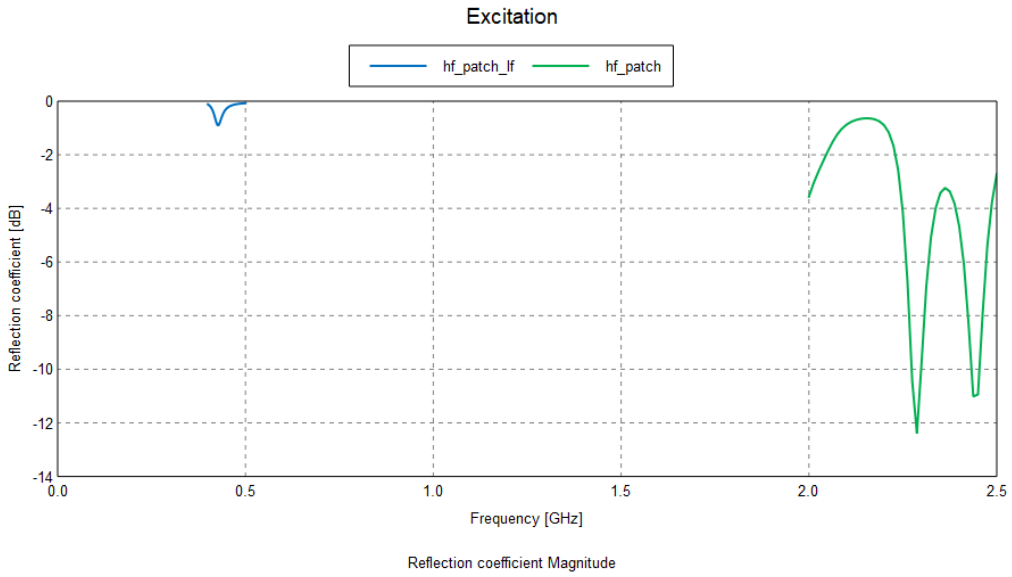

Figure 45: This is a graph of the reflection coefficient of the high frequency antenna over the full relevant frequency spectrum. It show a low reflection coefficient at the high frequency target but not at the low frequency target.

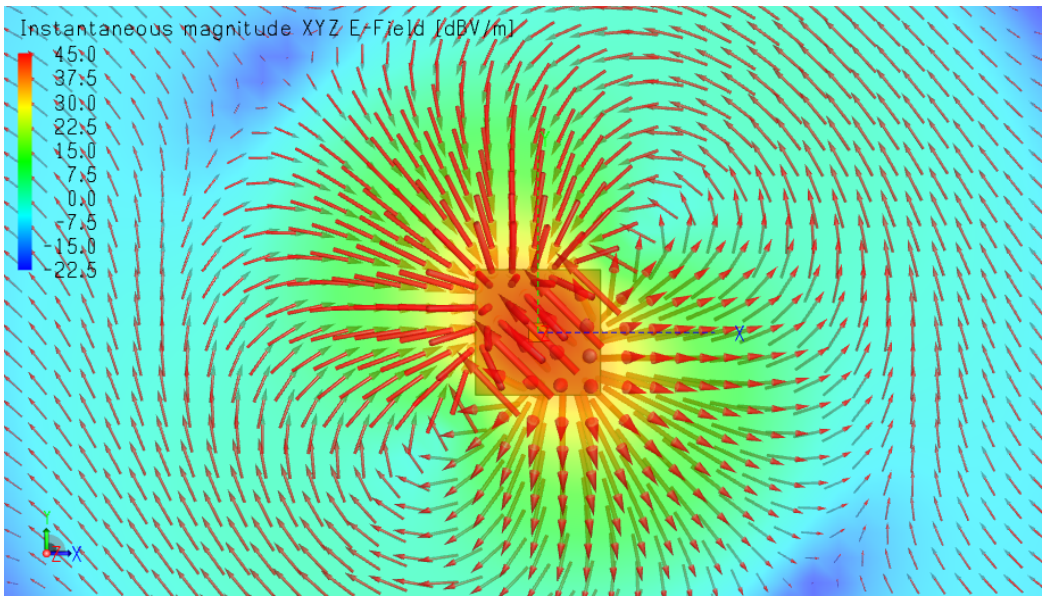

Figure 46: This is a plot of the near-field electric field of the high frequency antenna at the low frequency target, 450 MHz. This field will determine the optimal position for the antenna to excite the desired current modes.

3.4.3 Antenna Positioning

Now that the near field of the antenna has been solved for and the current distribution of the desired modes are known, all that remains is to position the antenna in a way that maximizes the interaction between the two. This position is unsurprisingly between the two solar panels so that currents along that edge will be excited. As stated in Section 3.2.5, the actual deployment and practicality of the antenna placement is out of scope of this thesis as the goal is to show how CMA can be used in the design process. The simulated antenna position was determined by the FEKO optimization tool based on the realized gain at 450 MHz.

The results of the antenna simulation show clear operation at 450 MHz where there wasn't operation before. Another difference worth noting is that with the introduction of the satellite, the main lobe from the antenna is deflected and no longer is the strongest broadside anymore. Figures 47 and 48 show how the lobes are more complex shapes and that the peaks for each target frequency are no longer perfectly aligned.

Figure 49 shows a relatively high realized gain at both operating frequencies for the main lobe of radiation. For comparison, Figure 50 shows the reflection coefficient of the design which also demonstrates resonate efficient operation at the target frequencies. It is also worth analyzing the MEC graph shown in Figure 51 which corresponds with the current distribution shown in Figure 52. Although the introduction of the patch changes the system and thus changes the modes so they are not the same as when calculated previously, mode 2 shows a current distribution that is significant at 450 MHz, has a strong current along the long edge of the solar panels, and has a relatively high MEC. This all reinforces the claim that the antenna has successfully coupled with the satellite body and is using the entire structure as the radiating element for the 450 MHz target frequency while still being able to operate

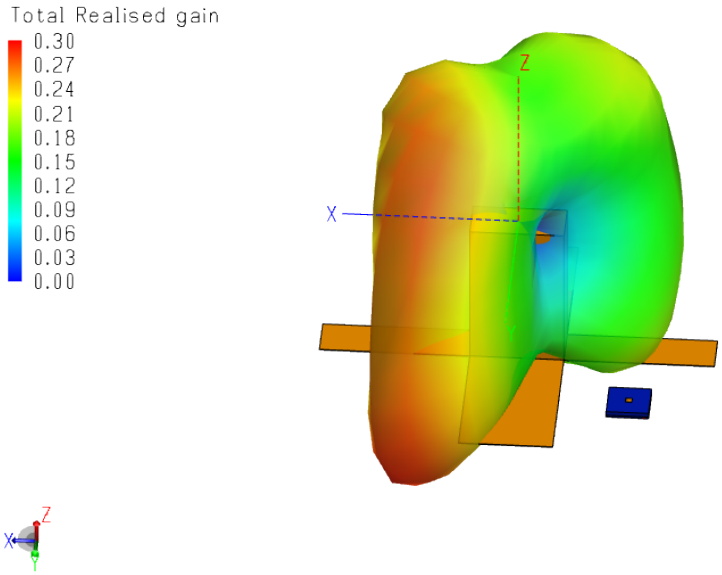

Figure 47: This is the far-field electric field of the high frequency antenna coupled with the CubeSat structure at the low frequency target, 450 MHz. The main lobe is not nadir pointing. If this design is utilize, other design factors for the overall project may have to be considered such as rotating the satellite during communication.

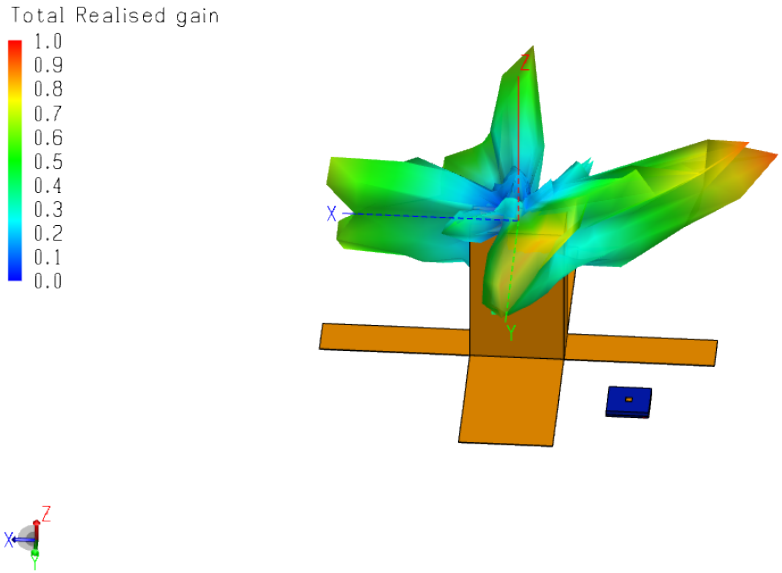

Figure 48: This is the far-field electric field of the high frequency antenna coupled with the CubeSat structure at the high frequency target, 2.285 GHz. It also does not have a main lobe that is nadir pointing which could introduce complications.

at its designed operational frequency of 2.285 GHz.

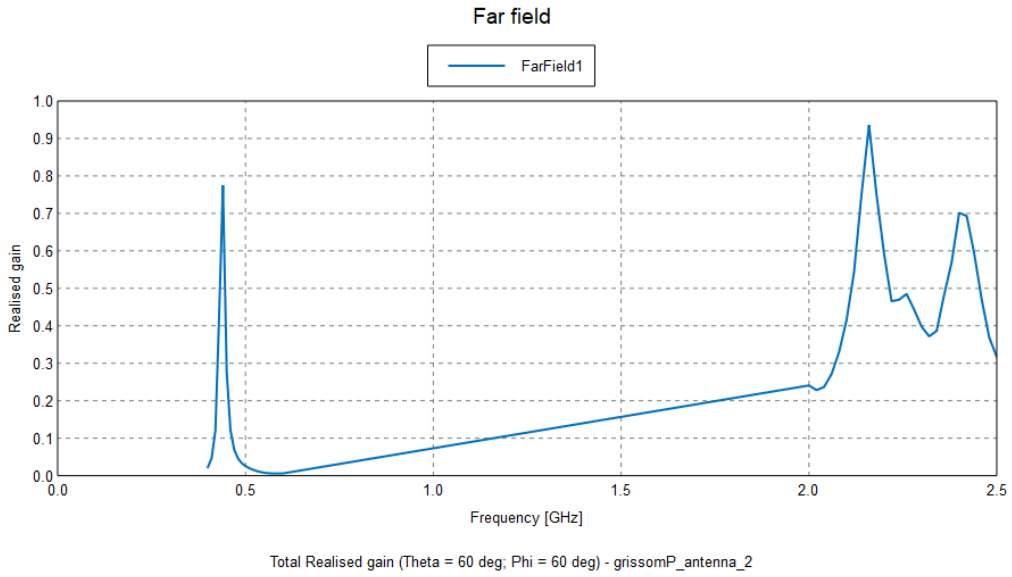

Figure 49: This is a plot of the realized gain of the high frequency antenna coupled with the CubeSat structure. It shows relative maximums at the two target frequencies indicating the design has met the requirements.

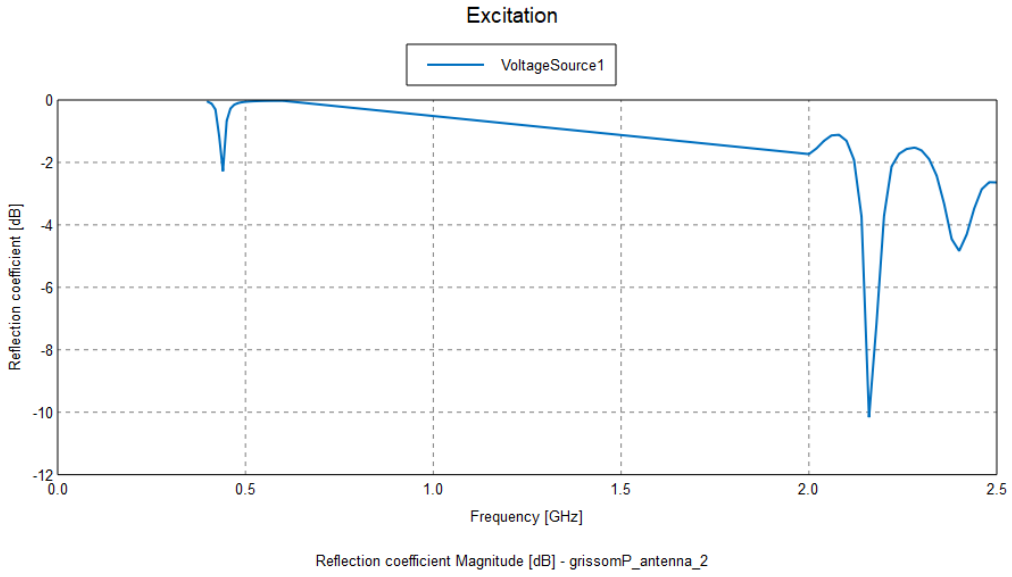

Figure 50: The reflection coefficient of the high frequency antenna coupled with the CubeSat structure. While the reflection coefficient at 450 MHz is not ideal for operation the fact their does exist a minimum supports the claims that are described in this section.

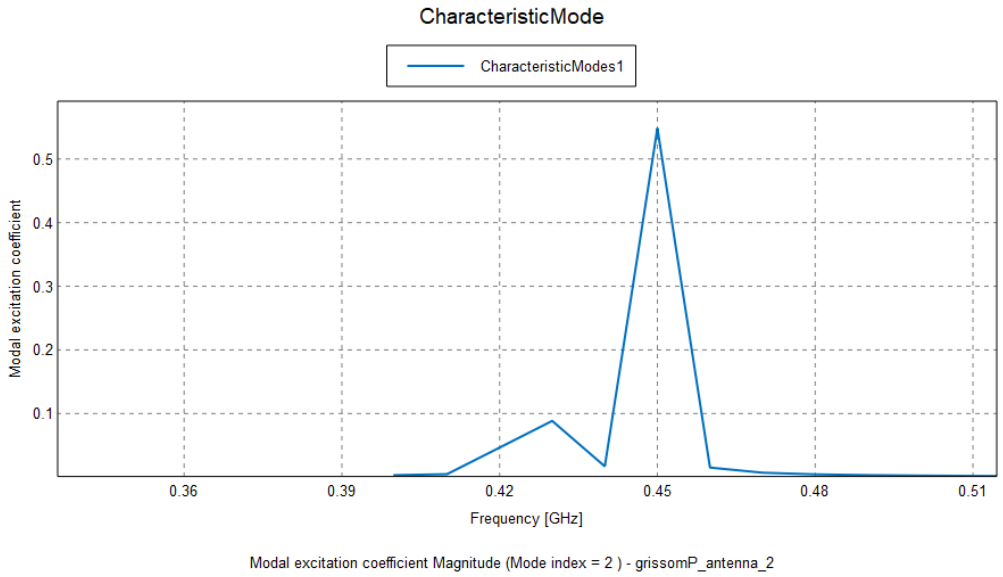

Figure 51: The MEC of the high frequency antenna coupled with the CubeSat structure at the lower frequency band. A mode is shown to be adequately excited at the target frequency.

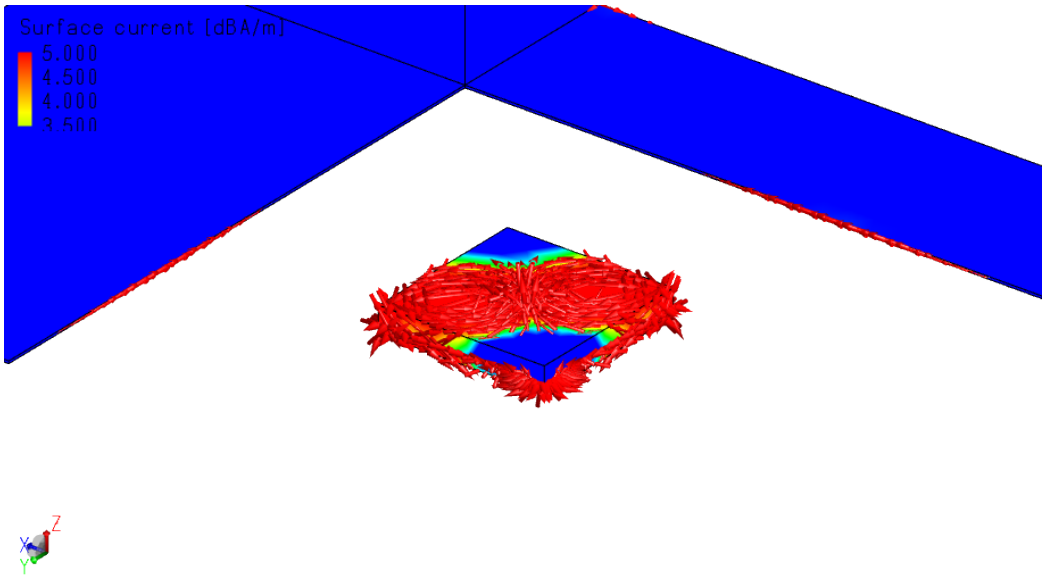

Figure 52: This is the current distribution of Mode Two of the Chassis Application at 450 MHz. Although much of the current resides on the patch where the source is, current is also visible along the solar panels. This indicates that current has been induced along the satellite body as designed.

IV. Results and Analysis

4.1 Introduction

This chapter will state the results and analysis of each application shown in III. Each application utilized Characteristic Modal Analysis (CMA) in a unique way and the degree to which it influenced the design is examined.

4.2 The Dipole Application

By far, the Dipole Application is the simplest application to analyze. It is relatively easy to implement as it is a straight conductive wire and no other materials are necessary. However, the main design issue with it is trying to operate at a low frequency of 450 MHz while optimizing the space required. Though the volume is small, the length of the dipole far exceeds 20 cm which will require creative deployment strategies for the Cube Satellite (CubeSat). If exceptions like these are allowable, then traditional antenna design techniques would work just as well. The analysis provided by CMA was possibly not necessary. That being said, CMA does influence the feed placement in a more elegant way than the common way utilized which usually involves an optimizer.

A center feed seems intuitive and is used in this method, but is not always optimal as shown in Section 3.2.5. CMA gives a good, insightful explanation for where the fed should be as opposed to using an optimizer to guess. This application only had two operating frequencies to optimize, but the method shown for source placement could easily identify the best source location if any of the requirements changed. The best area for improvement with this application is the initial antenna shape. CMA is dependent on an existing geometry so it cannot be used to synthesize a geometry and can only provide insight once a geometry is determined.

4.3 The Metasurface Application

The Metasurface Application is far more complex and difficult to model. It has many different dimensions, all of which can have a large impact on the performance if not manufactured precisely. The solution is also modeled with material of a calculated relative permittivity that may be difficult to implement in reality. However, this application does provide a compact solution that is less restricted in placement than the Chassis Application.

CMA was used to give good insight into how the antenna model was operating. Similar to the Dipole Application though, the greatest downfall to utilizing CMA in the design process is that it cannot provide insight into designing the initial geometry. It could be argued that the insight provided by CMA after the initial geometry is modeled can give the designer knowledge about designing they previously didn't have, but it still does not actively influence the conception of the initial geometry for a given set of requirements. This fact is clear with this application because the antenna model was mostly operating within the requirements before the CMA was even performed. However, if the requirements were different, it was shown in Section 3.3 that CMA could be used in suppressing certain modes by tailoring the metasurface design. This thesis antenna may not have demonstrated the use of CMA to design a metasurface, but it did bring up the potential ways the results of CMA could be applied given different requirements.

4.4 The Chassis Application

The Chassis Application trades the requirement of operating at a low frequency with that of a placement and near field requirement. This application is dependent on the mounting structure and as such requires it remains static during operation. This also makes this design less interchangeable and more specialized. It also requires

the antenna to be in a specific placement which may or may not be practical.

Unlike the other applications, the Chassis Application is only viable with the use of CMA. CMA on the mounting structure is needed immediately to re-define the requirements for the antenna. An optimizer cannot determine if a structure has the ability to radiate in a desired way, and thus this technique is only viable with the use of CMA in the design process. Additionally, CMA is necessary to determine the field needed by the antenna and then the best position to place it. This application may have more restrictions and complications than the others, but it is a viable method for operating at lower frequencies with a smaller antenna.

V. Conclusions

5.1 Conclusion

The goal of this thesis was to present three different viable antenna solutions to the AFIT Satellite Antenna problem which apply Characteristic Modal Analysis (CMA) principles in the design process. The purpose was to provide insightful strategies for the antenna design process of the AFIT Satellite to ensure the best design possible. It showed three different applications for the antenna problem, each of which succeeded in meeting the requirements. They also each emphasized a unique application of CMA that influenced the design process.

5.2 Future Work

This thesis utilized some properties of CMA to propose three antenna solutions that may be viable for the AFIT Satellite mission but there is more that could be done to extend this work. The Dipole Application could be extended by experimenting with top loading the ends. This can be done in a way that would shorten the length of the antenna and possible introduce some coupling with the solar panels. An aperture coupled feed patch antenna was the base design for both the Metasurface Application and the Chassis Application because of prior works. Other base antenna designs could be considered and may have better performance. This work could also be extended by either creating or obtaining pre-existing software that can optimally determine feed placement based on the current distributions solved for with CMA. Also, a more detailed model of the AFIT Cube Satellite (CubeSat) structure itself would not only add to the legitimacy of proposed antenna solutions but may also reveal that certain modal current distributions are more dominate than others and may be leveraged in design.

Bibliography

1. Robert J. Garbacz and Richard H. Turpin. A Generalized Expansion for Radiated and Scattered Fields. *IEEE Transactions on Antennas and Propagation*, 19(3):348–358, 1971.

2. Rainee N. Simons and Kavita Goverdhanam. Applications of nano-satellites and cube-satellites in microwave and rf domain. In *2015 IEEE MTT-S International Microwave Symposium*, pages 1–4, 2015.

3. Constantine A Balanis. *Antenna theory*. Wiley, 4 edition, 2016.

4. Pete Bevelacqua. The antenna theory website, 2021.

5. *feko comprehensive electromagnetic solutions*$_2$022. $EMSoftwareSystems - S.A.(Pty)Ltd, 7edition, 2014$.

6. *cst microwave studio 2016*. CST - Computer Simulation Technology AG, 2016.

7. Yikai Chen and Chao-Fu Wang. *Charasteristic modes*. Wiley, 2016.

8. Kin-Lu Wong. *Compact and broadband microstrip antennas*. Wiley, 2002.

9. Feng Han Lin and Zhi Ning Chen. Low-Profile Wideband Metasurface Antennas Using Characteristic Mode Analysis. *IEEE Transactions on Antennas and Propagation*, 65(4):1706–1713, 2017.

10. Karl F Warnick. *Numerical methods for engineering*. SciTech, 2011.

11. Yi Zhao, Xu Yao, and Chun yu Wang. Low-profile circularly polarized metasurface antenna with tailored reflection phase. *Electronics Letters*, 57(4):161–163, 2021.

12. Yue Juan, Wanchen Yang, and Wenquan Che. Communication. 67(5):3527–3532, 2019.

13. Francesco Alessio Dicandia and Simone Genovesi. Characteristic Modes Analysis of Non-Uniform Metasurface Superstrate for Nanosatellite Antenna Design. *IEEE Access*, 8:176050–176061, 2020.

14. Teng Li and Zhi Ning Chen. A dual-band metasurface antenna using characteristic mode analysis. *IEEE Transactions on Antennas and Propagation*, 66(10):5620–5624, 2018.

15. Feng Han Lin and Zhi Ning Chen. A Method of Suppressing Higher Order Modes for Improving Radiation Performance of Metasurface Multiport Antennas Using Characteristic Mode Analysis. *IEEE Transactions on Antennas and Propagation*, 66(4):1894–1902, 2018.

16. E. H. Newman. Small Antenna Location Synthesis Using Characteristic Modes. *IEEE Transactions on Antennas and Propagation*, 27(4):530–531, 1979.

17. Martin Vogel, Gopinath Gampala, Daniël Ludick, Ulrich Jakobus, and C. J. Reddy. Characteristic Mode Analysis: Putting Physics back into Simulation. *IEEE Antennas and Propagation Magazine*, 57(2):307–317, 2015.

Acronyms

CMA Characteristic Modal Analysis. iv, 2, 3, 4, 5, 7, 8, 9, 10, 11, 12, 15, 18, 19, 20, 21, 23, 24, 25, 26, 27, 28, 34, 35, 38, 40, 44, 47, 51, 59, 63, 64, 65, 66

CubeSat Cube Satellite. viii, ix, 1, 3, 27, 38, 40, 49, 50, 51, 54, 60, 61, 62, 63, 66

MEC Modal Excitation Coefficient. viii, x, 17, 19, 27, 31, 32, 33, 35, 36, 44, 54, 59, 62

MoM Method of Moments. 8, 9, 11, 12, 16

MS Modal Significance. viii, ix, 17, 18, 19, 26, 27, 29, 30, 33, 35, 44, 51, 52, 54

MWC Modal Weighting Coefficient. viii, ix, 17, 27, 32, 33, 34, 35, 36, 37, 44, 45, 46

PEC Perfect Electrical Conductor. 5, 11, 38, 51

REPORT DOCUMENTATION PAGE

Form Approved
OMB No. 0704–0188

1. REPORT DATE *(DD–MM–YYYY)*	2. REPORT TYPE	3. DATES COVERED *(From — To)*
06–02–2022	Master's Thesis	Sept 2020 — Mar 2022

4. TITLE AND SUBTITLE

Utilization of Characteristic Modal Analysis for the Antenna Design Needed for an AFIT Satellite

5a. CONTRACT NUMBER

5b. GRANT NUMBER

5c. PROGRAM ELEMENT NUMBER

6. AUTHOR(S)

Scott C. Podlogar

5d. PROJECT NUMBER

5e. TASK NUMBER

5f. WORK UNIT NUMBER

7. PERFORMING ORGANIZATION NAME(S) AND ADDRESS(ES)

Air Force Institute of Technology
Graduate School of Engineering and Management (AFIT/EN)
2950 Hobson Way
WPAFB OH 45433-7765

8. PERFORMING ORGANIZATION REPORT NUMBER

AFIT-ENG-MS-22-M-056

9. SPONSORING / MONITORING AGENCY NAME(S) AND ADDRESS(ES)

Intentionally Left Blank

10. SPONSOR/MONITOR'S ACRONYM(S)

11. SPONSOR/MONITOR'S REPORT NUMBER(S)

12. DISTRIBUTION / AVAILABILITY STATEMENT

DISTRIBUTION STATEMENT A:
APPROVED FOR PUBLIC RELEASE; DISTRIBUTION UNLIMITED.

13. SUPPLEMENTARY NOTES

14. ABSTRACT

Antenna design is a pervasive knowledge base for electrical engineers. As the number of new materials and techniques increase, so too do the demand and requirements pushing forth new innovative ideas to expand the capabilities antennas can achieve. Characteristic Modal Analysis (CMA), originally credited to Garbacz and Turpin, is a leading edge analytic technique that is one of these ideas. CMA breaks down the current distribution along a structure in a way that can offer great insights into how that structure operates as an antenna. This technique has great merits in post design analytics and can be integrated into the design process. This thesis applies the techniques of CMA to create independent designs for a single antenna problem involving a AFIT Satellite. The results are three different designs that meet the requirements proving the utility of CMA in the antenna design process for this specific application.

15. SUBJECT TERMS

Characteristic Modal Analysis, Cube Sat, Dual Frequency, Micro-strip Antenna

16. SECURITY CLASSIFICATION OF:			17. LIMITATION OF ABSTRACT	18. NUMBER OF PAGES	19a. NAME OF RESPONSIBLE PERSON
a. REPORT	b. ABSTRACT	c. THIS PAGE			Captain Scott C. Podlogar, AFIT/ENG
U	U	U	UU	82	19b. TELEPHONE NUMBER *(include area code)* (303) 888-1518; scott.podlogar@spaceforce.mil